AN ABSTRACT OF THE THESIS OF

Tim B. Link for the degree of Master or Science in Civil Engineering presented on June 12, 2014

Title: Seismic Performance of Reinforced Concrete Bridge Columns Constructed with Grade 80 Reinforcement

Abstract approved:

David Trejo and Andre R. Barbosa

The research presented in this thesis assessed the use of high strength steel (HSS) reinforcement for use in reinforced concrete (RC) bridge columns. HSS is not currently allowed in reinforced concrete bridge columns due to a lack of information on the material characteristics and performance information when used in RC bridge columns. Potential benefits in construction, performance, and economics justify the need for research. This research investigated the performance of HSS (ASTM A706 Grade 80 reinforcement) embedded in half-scale RC bridge columns. Column design followed standard design methodologies used by federal and state highway agencies. Six columns were subjected to lateral cyclic loadings, three columns were constructed with Grade 60 reinforcement and three columns were constructed with Grade 80 reinforcement. Results indicate that the columns constructed with Grade 80

reinforcement achieved similar resistances and displacement ductility values when compared with the reference columns constructed with Grade 60 reinforcement. The columns constructed with Grade 60 reinforcement showed larger hysteretic energy dissipation and typically exhbitied larger curvature ductility values than the columns constructed with Grade 80 reinforcement. The effects of the longitudinal reinforcement ratio and moment-shear span ratio on column performance were similar between columns constructed with Grade 60 reinforcement and columns constructed with Grade 80 reinforcement. The results from this research present a promising step towards the implementation of Grade 80 reinforcement in the design and construction of RC bridge columns, within the bounds of the variables used in the testing program.

Seismic Performance of Reinforced Concrete Bridge Columns Constructed with Grade 80 Reinforcement

by
Tim B. Link

A THESIS

Submitted to

Oregon State University

In partial fulfillment of

the requirements for the

degree of

Master of Science

Presented June 12, 2014

Commencement June 2014

Master of Science thesis of Tim B. Link presented on June 12, 2014.

APPROVED:

_____

Co-Major Professor, representing Civil Engineering

_____

Co-Major Professor, representing Civil Engineering

_____

Head of the School Civil and Construction Engineering

_____

Dean of the Graduate School

I understand that my thesis will become part of the permanent collection of Oregon State University libraries. My signature below authorizes release of my thesis to any reader upon request.

_____

Tim B. Link, Author

ACKNOWLEDGEMENTS

First and foremost I would first like to thank my advisors Dr. David Trejo and Dr. Andre R. Barbosa for taking me on as their graduate research assistant and for their continued guidance throughout my project. Also, I would like to thank Dr. Burkan Isgor and Dr. Roberto Albertani for being on my thesis committee and providing valuable input on my thesis.

I would also like to thank my parents (Mark and Jill Link), siblings (Rachel and Jack), and girlfriend (Liz Finley) for all of their love and support, without them I would not be the person that I am today.

Thank you to Oregon Department of Transportion and PacTrans for their funding of this project.

As with all projects, the success of the project is dependent on many dedicated people. I would like to thank Michael Dyson, James Batti, and Manfred Dittrich for their assistance in fabricating and testing the specimens. Students that assisted with the project include Jiaming Chen, Nicolas Matus, Greg Hendrix, Cody Tibbits, Lapyote Prasittisopin, Yicheng Long, Frank Porter, Amy Kordoska, and Drew Nielson. The assistance of Dana Ainsworth, my expert in all things financial, is duly noted. The assistance of Farwest Steel (Eugene, OR) for assisting with the fabrication of the reinforcement is greatly appreciated. Special thanks to Thomas Murphy and Dennis

Lauber from Cascade Steel (McMinnville, OR) for producing a special heat of the Grade 80 reinforcement. I sincerely thank all those that assisted with the project.

CONTRIBUTION OF AUTHORS

Dr. David Trejo is the principal investigator of this research project. Dr. Andre R. Barbosa is the co-principal investigator of this research project. Both Dr. David Trejo and Dr. Andre R. Barbosa are co-authors of both manuscripts presented in this thesis.

TABLE OF CONTENTS

Page

Chapter 1 INTRODUCTION 1

Chapter 2 INFLUENCE OF REINFORCEMENT GRADE AND LONGITUDINAL RATIO ON SEISMIC PERFORMANCE OF GRADE 80 RC COLUMNS 2

2.1 ABSTRACT 3

2.2 INTRODUCTION AND BACKGROUND 4

2.3 RESEARCH SIGNIFICANCE 10

2.4 EXPERIMENTAL PLAN AND PROCEDURE 10

2.4.1 Instrumentation 12

2.4.2 Test Setup and Testing Procedure 14

2.5 TEST RESULTS AND ANALYSIS 15

2.5.1 Overview 15

2.5.2 Steel Reinforcement Strains 16

2.5.3 Column Capacity 18

2.5.4 Column Ductility 20

2.5.5 Energy Dissipation 22

2.6 SUMMARY AND CONCLUSIONS 23

2.7 REFERENCES 25

TABLE OF CONTENTS (Continued)

Page

2.8 ACKNOWLEDGMENTS 27

2.9 TABLES AND FIGURES 28

2.9.1 List of Tables: 28

2.9.2 List of Figures: 28

Chapter 3 SEISMIC PERFORMANCE OF HIGH STRENGTH STEEL RC BRIDGE COLUMNS 35

3.1 ABSTRACT 36

3.2 INTRODUCTION 37

3.3 EXPERIMENTAL PLAN AND PROCEDURE 41

3.3.1 Test Specimen Design 42

3.3.2 Construction Sequence 44

3.3.3 Instrumentation 44

3.3.4 Test Setup and Testing Procedure 46

3.4 TEST RESULTS AND ANALYSIS 47

3.4.1 Steel Reinforcement Strains 47

3.4.2 Column Capacity 49

3.4.3 Column Ductility 51

TABLE OF CONTENTS (Continued)

Page

3.4.4 Energy Dissipation 54

3.5 SUMMARY AND CONCLUSIONS 56

3.6 REFERENCES 58

3.7 ACKNOWLEDGEMENTS 60

3.8 TABLES AND FIGURES 61

3.8.1 List of Tables 61

3.8.2 List of Figures 61

Chapter 4 GENERAL CONCLUSION 68

BIBLIOGRAPHY 71

LIST OF FIGURES

Figure Page

Figure 2.1 (a) Columns G60-1, G80-1, G60-2 and G80-2 cross-sections (b) test specimen geometry of G60-1, G80-1, G60-2 and G80-2 31

Figure 2.2 Columns G60-1, G80-1, G60-2 and G80-2 internal instrumentation 31

Figure 2.3 Columns G60-1, G80-1, G60-2 and G80-2 external instrumentation (NTS = not to scale) 32

Figure 2.4 Loading profile of columns G60-1, G80-1, G60-2 and G80-2 32

Figure 2.5 Photograph of column G80-1 crack mapping and concrete spalling 33

Figure 2.6 Shear force versus drift ratio of columns: (a) G60-1 and G80-1, (b) G60-2 and G80-2 33

Figure 2.7 Cumulative energy dissipation 34

Figure 3.1 (a) Columns G60, G80, G60-s, and G80-s cross-sections (b) test specimen geometry of columns G60, G80, G60-s, and G80-s 64

Figure 3.2 Column G60-s & G80-s internal instrumentation 64

Figure 3.3 Column G60-s & G80-s external instrumentation (NTS = not to scale) 65

Figure 3.4 Loading Profile of columns G60, G80, G60-s, and G80-s 65

Figure 3.5 Shear force versus drift ratio of columns G60-s and G80-s 66

Figure 3.6 Shear force versus drift ratio of columns: (a) G60 and G60-s, (b) G80 and G80-s 66

Figure 3.7 Cumulative energy dissipation of columns G60, G80, G60-s, and G80-s 67

LIST OF TABLES

Table Page

Table 2.1 Experimental test matrix of columns G60-1, G80-1, G60-2 and G80-2.....29

Table 2.2 Loading profile of columns G60-1, G80-1, G60-2 and G80-2 29

Table 2.3 Columns G60-1, G80-1, G60-2 and G80-2 capacities.....30

Table 2.4 Summary of ductility values of columns G60-1, G80-1, G60-2 and G80-2 30

Table 2.5 Energy dissipation of columns G60-1, G80-1, G60-2 and G80-2 30

Table 3.1 Experimental test matrix of columns G60, G80, G60-s, and G80-s 62

Table 3.2 Loading profile of columns G60, G80, G60-s, and G80-s.....62

Table 3.3 Columns G60, G80, G60-s, and G80-s capacities 63

Table 3.4 Summary of columns G60, G80, G60-s, and G80-s ductility values.....63

Table 3.5 Energy dissipation of columns G60, G80, G60-s, and G80-s.....63

Chapter 1 INTRODUCTION

Although high strength steel (HSS) reinforcement is commercially available, its use is limited. Potential benefits in construction, performance, and economics justify the need for research. Current codes do not allow HSS reinforcement in structural members designed to form plastic hinges (i.e., bridge columns). In general, higher strength steels exhibit lower ductility. However, Grade 80 (80 ksi [550 MPa]) reinforcement meeting American Society for Testing and Materials (ASTM) A706 requirements has been reported to have adequate ductility. Even with these reports, there is an overall lack of data on the performance of reinforced-concrete (RC) members constructed with Grade 80 reinforcement. Therefore, the objective of this study is to assess the behavior of circular reinforced-concrete bridge columns constructed with Grade 80 reinforcement meeting ASTM A706 specifications subjected to reversed cyclic lateral loading.

In this thesis a total of six columns were analyzed to determine the effects of the grade of reinforcement, effect of the longitudinal reinforcement ratio, and the effect of the moment-shear span ratio (aspect ratio) on column performance. The first manuscript (Chapter 2) evaluates the effect of the grade of reinforcement on column performance as well as the effect of the longitudinal reinforcement ratio on column performance. The second manuscript (Chapter 3) also evaluates the effect of the grade of reinforcement on column performance and evaluates the effects of the moment-shear span ratio on column performance.

Chapter 2 INFLUENCE OF REINFORCEMENT GRADE AND LONGITUDINAL RATIO ON SEISMIC PERFORMANCE OF GRADE 80 RC COLUMNS

Will be submitted to:

ACI Structural Journal

American Concrete Institute

38800 Country Club Dr.

Farmington Hills, MI 48331

2.1 ABSTRACT

The use of high strength steel (HSS) reinforcement for use in reinforced-concrete (RC) bridge columns is currently not allowed due to a lack of information on material characteristics and seismic performance when embedded in structural concrete members. However, HSS reinforcement could provide economic benefits and improved constructability. Potential benefits in improved constructability and/or reduced material quantities justify further research on RC columns constructed with HSS reinforcement. As such, this research investigated the performance of Grade 80 (minimum yield strength of 80 ksi [550 MPa]) HSS reinforcement embedded in RC bridge columns. The HSS reinforcement met the American Society for Testing and Materials (ASTM) A706 requirements. Four columns were tested: two constructed with ASTM A706 Grade 60 reinforcement and two constructed with ASTM A706 Grade 80 reinforcement. The columns were subjected to lateral cyclic loading to determine the effects of the reinforcement grade and the effect of the longitudinal reinforcement ratio on the performance of RC circular bridge columns. Results indicate that the columns constructed with Grade 80 HSS reinforcement achieved similar resistances as well as maximum drifts, with minimal reductions in curvature ductility values when compared with the reference columns constructed with Grade 60 reinforcement. Results also indicate that the effect of the longitudinal reinforcement ratio on column performance is similar for columns constructed with either Grade 60 or Grade 80 reinforcement. However, columns constructed with Grade 80

reinforcement exhibited lower energy dissipation than the reference columns constructed with Grade 60 reinforcement.

Keywords: ASTM A706 Grade 80; circular columns; cyclic tests; high-strength reinforcing steel; longitudinal reinforcement ratio; reinforced concrete bridge columns; seismic performance

2.2 INTRODUCTION AND BACKGROUND

Although ASTM A706 Grade 80 reinforcement is commercially available, its use in practice today is still limited. Bridge and building design codes in the United States (US) have limited the nominal yield strength of reinforcement to 75 ksi (520 MPa). However, in 2011, the American Association of State Highway and Transportation Officials (AASHTO) began allowing the use of HSS reinforcement with nominal yield strengths up to 100 ksi (690 MPa), but only for sections that are not expected to form plastic hinges (e.g., not bridge columns). The primary reason for limiting the use of HSS reinforcement is because increasing the yield strength typically results in decreased ductility when compared to Grade 60 reinforcement, even though Grade 80 reinforcement meets the ASTM A706 ductility requirements (ASTM 2009). There is an overall lack of data on the performance of RC compression members constructed with Grade 80 reinforcement that can form plastic hinges, thus Grade 80 reinforcement is not allowed in all RC members. In addition designers are reluctant to specify this material because of potential errors in placement that may arise due to the

presence of more than one reinforcement grade, i.e., placing Grade 60 reinforcement where Grade 80 reinforcement is required.

The main objective of this study is to generate data on the performance of circular RC bridge columns constructed with Grade 80 reinforcement subjected to reversed cyclic lateral loading. This research will provide seminal data to support State Highway Agencies (SHAs) in their design of bridges constructed with Grade 80 reinforcement. In this study, an experimental plan was developed to assess the effects of reinforcement grade (yield strength) and longitudinal reinforcement ratio on column performance.

The evolution of the development of reinforcement steel grade is worth reviewing. This review can provide information on why Grade 80 reinforcement is not used in RC bridge columns in the US, even though similar reinforcement is currently used in seismically prone regions of the world, such as New Zealand and a few European countries. The first specifications in the US for concrete reinforcement were developed by the American Association of Steel Manufacturers in 1910 (Concrete Reinforcing Steel Institute 2001). The following year ASTM adopted the standard specification A15 for billet steel reinforcement, which required a yield strength of 33,000 psi (228 MPa) for structural grade reinforcement. The standard specification A15 was in effect for many years. However, in 1959 ASTM developed new specifications for concrete reinforcement for nominal yield strengths of 60 ksi (414 MPa) and 75 ksi (520 MPa) (Gustafson 2010). As early as 1967 engineers began

recognizing the potential benefits of HSS reinforcement. Specifically, reports identified that Grade 80 reinforcement could be economically used and produced and that if produced they would be in demand (Gustafson 2010). Several decades later Grade 80 reinforcement made its way into the standards, but has not yet been widely accepted or used. This is likely a result of the Grade 80 reinforcement not being allowed in plastic hinge regions, but also of lack of interest at this time from the producers in lobbying for its use, because it is not expected that the price per unit weight would be substantially different than Grade 60 reinforcement while the nominal yield strength to unit weight is increased by 33 percent. However, currently there is a renewed interested from the producers and DOT's for the use of Grade 80 reinforcement.

One of the first investigations on structural elements constructed with Grade 80 reinforcement was reported by Rice and Gustafson (1976). The authors analytically assessed the moment capacity of structural elements constructed with Grade 80 reinforcement. Using moment interaction diagrams the authors showed that columns constructed with Grade 80 reinforcement exhibited a significant increase in moment capacity compared to columns constructed with Grade 60 reinforcement. The authors also conducted an economic analysis and reported that the use of Grade 80 reinforcement could have a significant reduction in cost if large quantities could be manufactured (Rice and Gustafson 1976). Even with such promising results, it is clear that the designers and the construction market were not ready for this material.

One potential benefit of using Grade 80 reinforcement could be to reduce reinforcement congestion while maintaining the same level of column performance as columns constructed with Grade 60 reinforcement. Reinforcement congestion can be a significant challenge, especially in seismic regions (Gustafson (2010); Risser and Hoffman (2014)). Rautenberg et al. (2010) reported that HSS reinforcement reduced bar congestion without significantly reducing the performance for RC columns with low axial loads. Test results indicated that columns constructed with conventional A615 Grade 60 and A1035 Grade 120 reinforcement both exhibited drift ratios exceeding 4 percent and both had similar moment capacities. Results indicated that as long as the fracture strain of the longitudinal reinforcement exceeded 7 percent for a reference gage length (8 inches [203 mm]) and the amount and detailing of the transverse reinforcement is adequate to prevent shear failure, bond failure, and bar buckling, then the amount of reinforcement can be reduced proportionally with the increase in yield strength. However, the authors reported a noticeable difference in hysteretic energy dissipation between the columns constructed with Grade 60 and Grade 120 reinforcement, but noted that the difference was a result of the difference in column stiffness. Even though the increased strength of each bar indicates that per bar a larger amount of energy is dissipated (Mander et al. 1994). If RC members containing Grade 80 reinforcement are designed and constructed to have the same capacity as columns constructed with Grade 60 reinforcement reducing the amount of reinforcement may result in reduced energy dissipation.

Another topic discussed by Rautenberg et al. (2010) is related to bar fracture and bar buckling. Rodriguez et al. (1990) investigated the effects of buckling in the reverse cyclic loading of steel reinforcement. The authors reported if insufficient tie spacing exists and if this is combined with large tension and compression strain reversals progressing into the inelastic range, buckling of the longitudinal reinforcement can occur during an earthquake (Rodriguez et al. 1999). This indicates that the increased yield strength of Grade 80 reinforcement may not be fully utilized due to potential effects of buckling, which controls the fracture strain under reversed cyclic loading. This paper will investigate these effects further.

As previously mentioned, one approach in the design of RC columns constructed with Grade 80 reinforcement is to maintain the design column capacity while reducing the amount of reinforcement when compared to the same column designed with Grade 60 reinforcement. Currently, AASHTO limits the minimum longitudinal reinforcing ratio to 1 percent when Grade 60 reinforcement is used; therefore there is the potential to use Grade 80 reinforcement ratios lower than 1 percent. Priestley and Benzoni (1996) investigated the seismic performance of circular columns with low longitudinal reinforcement ratios. One column had the minimum longitudinal reinforcement ratio of 1 percent and one column had a longitudinal reinforcement ratio of 0.5 percent. The authors reported that the column with a longitudinal reinforcement ratio of 0.5 percent exhibited a ductile response, adequate distribution of flexural cracking, and failed with an associated displacement ductility, μ_{Δ}, of 10 due to shear failure. The maximum drift angle was reported to be 2.6 percent. The authors also reported that failure of columns

with 1.0 percent longitudinal reinforcement ratio was due to shear. The authors concluded that the results confirmed analytical predictions that 0.5 percent reinforcement ratio can safely be used as the lower longitudinal reinforcement ratio for RC columns subjected to low axial loads. This conclusion could prove critical to implementing Grade 80 reinforcement because current codes limit the minimum ratio to 1.0 percent. This paper addresses this question.

Although there are potential benefits in using Grade 80 reinforcement, significant questions still exist. The main objective of this paper is to answer some of those questions through the comparison of the experimental behavior of four RC columns. Two columns are constructed with ASTM A706 Grade 80 reinforcement and other two columns are constructed with ASTM A706 Grade 60 reinforcement. In terms of performance, the focus is placed on the maximum lateral drifts and the tested moment capacity. Secondary topics are also addressed herein. First, the energy dissipation of RC systems containing Grade 80 reinforcement is not well defined and comparisons between the Grade 60 and Grade 80 columns are presented and discussed. Second, to achieve optimal benefits of Grade 80 reinforcement, the current minimum reinforcement ratio may have to be reduced and fall below the prescribed 1 percent minimum longitudinal reinforcement ratio. One specimen constructed with Grade 80 has a longitudinal reinforcement ratio that is less than 1 percent. Lastly, the potential pros and cons of using Grade 80 reinforcement in cyclic loading applications are assessed and quantified.

2.3 RESEARCH SIGNIFICANCE

ASTM A706 Grade 80 reinforcement used in RC bridge columns could result in lower quantities of reinforcement and reduced congestion if research results can show similar and safe performance when compared to columns constructed with ASTM A706 Grade 60 reinforcement. This research reports on experimental testing of four circular RC columns constructed with either Grade 80 or Grade 60 reinforcement meeting ASTM A706 requirements. This paper evaluates and compares the performance of circular RC columns constructed with Grade 60 and Grade 80 reinforcements. This information can be used to assess the potential use of Grade 80 reinforcement in seismic areas.

2.4 EXPERIMENTAL PLAN AND PROCEDURE

An experimental program was developed to assess the performance of RC columns constructed with Grade 80 reinforcement meeting ASTM A706 specifications when subjected to cyclic loading. The experimental program consisted of testing four half-scale circular RC bridge columns. Two of the columns were designed and constructed with Grade 80 reinforcement and the remaining two columns were designed and constructed with Grade 60 reinforcement also meeting ASTM A706 specifications. In addition, to the reinforcement grade, the effect of the longitudinal reinforcement ratio was evaluated.

The 2-foot (0.61 m) diameter columns were 12 feet (3.66 m) tall measured from the top of the footing to the axis of the actuator. This corresponds to a half-scale specimen

of a typical 4-foot (1.22 m) diameter column built in Western US, including California, Oregon, and Washington. The total weight of the columns, including the RC load stub (header) and footing, was 10.45 (short-U.S.) tons (9.48 metric tonnes). The specimens are representative of a bridge containing a single pier loaded in the transverse direction and were tested as cantilever columns with a moment-shear span ratio of 6. Figure 2.1(a) shows the cross-sections of the columns tested and Figure 2.1(b) shows the geometry of the columns tested. Note that the external dimensions of the columns are identical for the four test specimens.

Table 2.1 shows the experimental plan. The first column, G60-1, was designed with ASTM A706 Grade 60 reinforcement with a longitudinal reinforcement ratio, ρ_l, of 1.11 percent (16 #5 bars = 16 ϕ16 mm bars) . The second column, G80-1, was designed to have the same capacity as G60-1, but was designed with ASTM A706 Grade 80 reinforcement. Thus, the longitudinal reinforcement ratio used was 0.80 percent (12 #5 bars = 12 ϕ16 mm bars). It is worth noting that the ratio of the number of bars is the same as the ratio of the nominal yield strength of both reinforcement grades. The third column, G60-2, was designed with a longitudinal reinforcement ratio, ρ_l, of 2.19 percent (22 #6 bars = 22 ϕ19 mm bars). The last column, G80-2, was designed to have approximately the same capacity as G60-2, but was designed with ASTM A706 Grade 80 reinforcement. This corresponded to a longitudinal reinforcement ratio, ρ_l, of 1.58 percent (16 #6 bars = 16 ϕ19 mm bars). Note that the increase in yield strength ratio did not perfectly match the decrease in the number of

longitudinal reinforcing bars ratio. The increase in yield strength ratio was 1.33 and the decrease in the number of longitudinal reinforcing bars ratio was 1.38. For all columns, the transverse reinforcement ratio, ρ_t, was designed to be 0.82 percent, which corresponded to a spiral pitch (spacing) of 2.50 inches (63.5 mm) on-center. The spiral reinforcement bar size was #3 (ϕ10 mm) for all columns. The grade of the transverse reinforcement was the same grade as the longitudinal reinforcement for each test column.

Concrete casting was done in two pours. First the footing was casted and then the column and load stub (header) were casted. Columns G60-1 and G80-1 were cast at the same time and so were columns G60-2 and G80-2. The concrete mixture contained a ⅜-inch (9.5 mm) maximum size aggregate (half scale of typical ¾-inch [19.1 mm]) and had a 28-day design concrete compressive strength of 4 ksi (28 MPa). The mixture was also proportioned to be pumpable and had a minimum required slump of 5 inches (127 mm). Additional specimen details can be found in the research report (Trejo et al. 2014).

2.4.1 Instrumentation

Each test specimen was instrumented to characterize and track indicators of performance of the columns during cyclic testing. Figure 2.2 shows the internal instrumentation plan. A total of 29 strain gages were placed on both the longitudinal reinforcement (22 strain gages) and the transverse reinforcement (7 strain gages). Strain gages on the longitudinal reinforcement were placed on the farthest northern

and southern reinforcement, i.e., in the direction of the applied lateral load. Two strain gages were placed at each location on the east and west sides of the northern and southern reinforcement in the region where significant inelastic strains were expected to develop, i.e. over the analytical plastic hinge length (24 inches [610 mm]). Single gages were placed outside of the analytical plastic hinge zone on the east side of the longitudinal reinforcement. Transverse strain gages were placed on the outer most surface of the spiral at approximately the same elevations as the strain gages on the longitudinal reinforcement. Location of the strain gages are shown in Figure 2.2, the lowest elevation is which strain gages were placed is referred to as level 1 and the highest elevation is referred to as level 7. Figure 2.3 shows the locations of the external instrumentation installed to measure displacements, load, and deformations. In total, 42 transducers were installed. Twenty (20) string potentiometers (label B) were placed to measure column rotations. These string potentiometers were attached to aluminum angles that were supported by and bolted to two ⅜-inch (9.5 mm) diameter threaded rods. The threaded rods were placed through the column, prior to casting, at five different elevations (two rods at the five levels; ten rods in total). The applied horizontal load was measured using a load cell (label G) in the actuator and the tip displacement was measured using a string potentiometer (label A) at the same elevation as the applied load. Details on additional instrumentation not presented in this report are provided in Trejo et al. (2014).

2.4.2 Test Setup and Testing Procedure

Once the footing, column and header were casted, the test setup initiated with stressing the column footing to the strong floor. The hydraulic actuator was then bolted to the RC header and lastly the axial load system was assembled. The axial load was applied with a hydraulic jack located between the top of the column header and a steel beam. The steel beam was tied into the column footing using prestressing threaded rods. The initial applied axial load was 90 kips (400 kN), corresponding to 5 percent of the nominal axial capacity of the column in compression. The test setup included a system to minimize fluctuations in axial loads. A concave plate and convex nut were used to allow rotation of the prestressing rod to minimize the fluctuation in the applied axial load. In addition, a pneumatic nitrogen accumulator was placed in series with the hydraulic jack.

Horizontal loading consisted of pushing and pulling the column (in the north-south direction) to predetermined displacement levels. Each displacement level consisted of three cycles (six peaks). Each cycle started at zero displacement, was then displaced in the positive direction towards the positive peak (North, pushed away from the strong wall), was then displaced in the negative direction towards the negative peak (South, pulled towards the strong wall), and finally returned back to zero displacement. This process was repeated three times for each predetermined displacement cycle. Figure 2.4 shows the loading profile and Table 2.2 shows the displacement cycles and loading rates for each displacement cycle.

To characterize the material properties of the concrete and steel reinforcement, several material tests were performed. For the concrete material, compressive strength (ASTM C39) tests (C09 Committee 2014a), splitting tensile strength (ASTM C496) tests (C09 Committee 2011), modulus-of-elasticity (ASTM C469) tests (C09 Committee 2014b), and modulus-of-rupture (ASTM C78) tests (C09 Committee 2010) were performed. Concrete samples were made and cured following ASTM C31 specifications (C09 Committee 2012). For the steel reinforcement, strength and strain parameters were obtained from tension tests performed using a 110-kip universal testing machine following ASTM E8 (E28 Committee 2013), E83 (E28 Committee 2010) and A370 (A01 Committee 2013) specifications.

Calculations were performed to remove the geometry effects of the applied axial load, which because of the experimental setup, is a follower load affecting the shear and moment capacity of the column. Details of these calculations are provided in Trejo et al. (2014).

2.5 TEST RESULTS AND ANALYSIS

2.5.1 Overview

Figure 2.5 shows a photograph of the crack mapping and a photograph of the concrete spalling near the end of the testing of column G60-2. Similar crack patterns were reported for all four columns. At large displacement cycles concrete spalling extended to an elevation approximately equal to one half of the column diameter for all of the columns. The failure mode was a flexural one for all of the columns. Longitudinal bar-

buckling followed by longitudinal bar facture was the main mode of failure observed. Column G80-1 was able to achieve a larger maximum tip displacement prior to failing when compared to column G60-1. The columns with an increase longitudinal reinforcement ratio (G60-2 and G80-2) both reached the same maximum tip displacement prior to failure, which was greater than columns (G60-1 and G80-1).

In the following subsections, the results of two pairs of columns (G60-1 and G80-1, G60-2 and G80-2) are compared to determine the effects of the steel reinforcement grade and the effect of longitudinal reinforcement ratio on the column performance. Steel reinforcement strains, column capacity, column ductility, and energy dissipation are compared in this paper.

2.5.2 Steel Reinforcement Strains

The yield strain value for each bar size and grade was determined from applying the 0.2 percent offset method on the experimental stress-strain data. The longitudinal reinforcement in column G60-1 yielded at a tip displacement of 1.17 inches (29.7 mm). This reinforcement yielding initially occurred at the base of the column (level 2) during the approach to the first peak of the 1.25-inch (31.8 mm) displacement cycle. The longitudinal reinforcement also yielded at levels 3 and 4 during this displacement cycle. The longitudinal reinforcement in column G80-1 yielded at a tip displacement of 1.52 inches (38.6 mm). This initially occurred at instrumentation level 3 during the approach to the first peak of the 2.50-inch (63.5 mm) displacement cycle. Note that this was one displacement cycle later than when yielding initially occurred for column

G60-1. The reinforcement at the base of the column, level 2, and through level 5 also yielded later in this same displacement cycle for column G80-1. The longitudinal reinforcement in column G80-1 initially yielded 6 inches (152 mm) above the base of the column while the longitudinal reinforcement in column G60-1 initially yielded at the base of the column. This may indicate that the development length is larger for the Grade 80 reinforcement and that bar slip may have been larger for the Grade 80 reinforcement. The longitudinal reinforcement in column G60-1 yielded in the footing (level 1) on the 3.75-inch (95.3 mm) displacement cycle and the longitudinal reinforcement in column G80-1 did not yield in the footing (level 1) until the 8.75-inch (222 mm) displacement cycle. It is worth noting, that the transverse reinforcement of columns G60-1 and G80-1 did yield.

The longitudinal reinforcement in column G60-2 yielded at a tip displacement of 1.44 inches (36.6 mm). This initially occurred at the base of the column, level 2, during the approach to the first peak of the 2.50-inch (63.5 mm) displacement cycle. The longitudinal reinforcement also yielded during this displacement cycle at all levels expect for level one which is inside the footing. Note that at level 7 only the southernmost longitudinal reinforcement yielded and the strain value was just slightly above the yield strain value. The longitudinal reinforcement in column G80-2 yielded at a tip displacement of 1.58 inches (40.1 mm). This initially occurred during the approach to the first peak of the 2.50-inch (63.5 mm) displacement cycle at the base of the column (level 2). The longitudinal reinforcement also yielded during this displacement cycle at levels 3 through 6. The longitudinal reinforcement in column

G60-2 yielded in the footing (level 1) on the 3.75-inch (95.3 mm) displacement cycle and the longitudinal reinforcement in column G80-2 never yielded in the footing (level 1). Again, results seem to indicate that development lengths may be larger for the Grade 80 reinforcement. All the transverse strains were small in magnitude and never approached yielding, except for column G80-2 at level 3 where on the final displacement cycle in which due to longitudinal bar buckling displaced the spiral vertically, being pushed away from the original position.

When comparing the effect of the longitudinal reinforcement ratio on the reinforcement strains, the two columns reinforced with Grade 60 (G60-1 and G60-2) were compared against the two columns reinforced with Grade 80 (G80-1 and G80-2). Column G60-2 yielded at a larger displacement cycle compared to G60-1 whereas both Grade 80 columns (G80-1 and G80-2) yielded during the same displacement cycle.

2.5.3 Column Capacity

Results of the following generalized column forces are discussed in this subsection. Column force results include the maximum applied force, shear force, and bending moment. Based on the comparison of the nominal moment capacities to the moment capacities obtained from the testing an overstrength factor is proposed.

Table 2.3 summarizes the column capacities. As shown in the table, the maximum applied force of columns G60-1 and G80-1 are very similar, and the maximum shear forces are identical. The percent difference between the expected moment capacities

of columns G60-1 and G80-1 is 1.00 percent. The percent difference between the tested moment capacities of columns G60-1 and G80-1 is 3.2 percent. The percent differences suggest that no special considerations are needed to predict the moment capacity of a concrete column constructed with Grade 80 reinforcement compared to a column constructed with Grade 60 reinforcement near the minimum longitudinal reinforcement ratio and with a moment-shear span ratio of six. The experimental data suggests that a column constructed with Grade 80 reinforcement can safely have a longitudinal reinforcement ratio of 0.83 percent. Figure 2.6(a) shows the shear force versus drift ratio for columns G60-1 and G80-1. It can be seen from this plot that the response of the two columns are similar except the unloading of column G80-1 dissipates less energy when compared to column G60-1.

Figure 2.6(b) shows the shear force versus drift ratio for columns G60-2 and G80-2. The differences in maximum applied force and maximum shear force between columns G60-2 and G80-2 was expected because the columns nominal moment capacity was slightly different. The difference in nominal moment capacity was due to being unable to exactly match the increase in yield strength of the longitudinal bars with the reduction of the number of longitudinal bars. The percent difference between the expected moment capacities of columns G60-2 and G80-2 is 3.29 percent, and the percent difference between the tested moment capacities of columns G60-2 and G80-2 is 9.81 percent. The percent differences suggest that special considerations may be needed to predict the moment capacity of a concrete column reinforced with Grade 80 reinforcement with a longitudinal reinforcement ratio near two percent, which are also

translated by the smaller overstrength factors for columns constructed with Grade 80 reinforcement.

As shown in Table 2.3 the increase in the longitudinal reinforcement ratio resulted in a larger computed overstrength factor for both columns constructed with Grade 60 reinforcement and for columns constructed with Grade 80 reinforcement. Figure 2.6(a) and 2.6(b) shows the shear force versus drift ratio up to the first longitudinal reinforcement bar fracture for columns G60-1 and G80-1 as well as G60-2 and G80-2, respectively. From these figures it can be seen that the overall shape of the hysteretic loops for Grade 80 columns are "thinner" and will thus result in smaller energy dissipation. This result is discussed in more detail below.

2.5.4 Column Ductility

Column ductility is analyzed herein in terms of displacement ductility and curvature ductility. The displacement ductility is computed as the ratio of the maximum column tip displacement to the column tip displacement at a reference yield of the column. Note that the reference yield of the column can be computed using different definitions. Herein, results for three different definitions of reference yield are presented. The definitions used are: (i) the displacement at first yield; (ii) the displacement at which the longitudinal reinforcement bars reach a strain of one percent; (iii) the curvature computed using equation 2.19a from Priestley (2003). The curvature ductility is computed as the ratio of the maximum curvature and the reference yield curvature (iii). The curvature ductility is computed at each of the five

curvature instrumentation levels, with level 1 corresponding to the curvature instrumentation at the lowest elevation and level 5 corresponding to the curvature instrumentation at the highest elevation.

Table 2.4 summarizes the displacement and curvature ductility values for the four columns. The results indicate that when using the displacement at the reference yield (ii) column G80-1 exhibited a larger displacement ductility value compared to column G60-1. However the displacement ductility is larger for column G60-1 when compared to column G80-1 when using the first yield (i). The displacement ductility values were larger for column G60-2 when compared to column G80-2 for both definitions of displacement reference yield. The percent difference between the displacement ductility values using the reference yield (ii) criteria between columns G60-2 and G80-2 is 5.15 percent. For both sets of columns the curvature ductility was largest closest to the base of the column and decreased as the elevation increased. For both columns constructed with Grade 60 reinforcement and columns constructed with Grade 80 reinforcement the increase in longitudinal reinforcement resulted in larger displacement and curvature ductility values. The magnitude of the increase was similar between the Grade 60 and Grade 80 columns other than the curvature ductility at level 2 where column G60-2 showed a significantly larger increase from column G60-1 compared to the increase between columns G80-2 and G80-1.

2.5.5 Energy Dissipation

The hysteretic energy dissipated was determined for each column. The value was determined by taking the area within the applied force versus displacement hysteretic loops for each displacement cycle. This was computed by numeric integration using the Simpson rule. It is worth noting that for each drift ratio cycle there was typically 3 cycles each having a north and south displacement peak equal to the value of the given displacement cycle. Table 2.5 summarizes the energy dissipated at first yield (i) and reference yield (ii) of the columns as well as the total energy dissipated up to the first longitudinal reinforcement fracture for the four columns. As shown in Table 2.5, column G60-1 exhibited greater energy dissipation prior to failure compared to column G80-1. This is most likely due to the reduction in the area of longitudinal reinforcement in column G80-2, which results in lower column stiffness, which in turn lowers its energy dissipation capacity. It can be seen in this table that column G80-1 dissipated more energy when compared to column G60-1 at the first yield (i) and the reference yield (ii) of the column. Figure 2.7 shows the cumulative energy dissipated up to the first reinforcement fracture for the four columns. As seen in Figure 2.7 column G60-1 was able to dissipate more energy after the reference yield (ii) of the column compared to column G80-1. As shown in Table 2.5 and Figure 2.7, column G60-2 exhibited greater energy dissipation when compared to column G80-2 throughout the testing. This is most likely due to the reduction in the area of reinforcement in column G80-2.

In summary, for both columns constructed with Grade 60 reinforcement and columns constructed with Grade 80 reinforcement, the increase in the longitudinal reinforcement ratio resulted in an increase in energy dissipation. This supports the claim by many authors in the literature that energy dissipation is a function of the amount of longitudinal reinforcement rather than the grade of reinforcement. It is worth noting that energy dissipation is not a primary parameter used in design, however it becomes an important parameter when predicting the performance of structures and also when modeling structures to collapse. It should be noted that most codes do not require a minimum energy dissipation value.

2.6 SUMMARY AND CONCLUSIONS

The use of Grade 80 reinforcement could reduce reinforcement quantities, could reduce reinforcement congestion, and could improve the constructability and economy of RC structures. However, limited research has been performed to validate the use of Grade 80 reinforcement. Results from a limited number of research projects indicate that Grade 80 reinforcement should be considered for use in all member types. This research assessed the performance of two pairs of columns, each pair consisting of one column constructed with Grade 60 reinforcement and the other constructed with Grade 80 reinforcement. A total of four columns were presented in this paper.

The main conclusions that can be drawn from these test results are:

1. Columns constructed with Grade 80 reinforcement achieved similar resistance, maximum displacement, and displacement ductility values when compared with the reference columns constructed with Grade 60 reinforcement;
2. Within the bounds of the parameters tested columns constructed with Grade 80 reinforcement with a longitudinal reinforcement ratio below one percent safely achieved adequate performance;
3. Columns constructed with Grade 60 reinforcement exhibited larger hysteretic energy dissipation than the columns constructed with Grade 80 reinforcement. However, by comparing the longitudinal reinforcement ratio of columns constructed with Grade 60 and Grade 80 reinforcement showed that the energy dissipation is a function of the amount of reinforcement rather than a function of the reinforcement grade, especially since the columns were designed to reach the same capacities;
4. The observed modes of failure for columns constructed with Grade 60 and Grade 80 reinforcement were similar. The main mode of failure was longitudinal reinforcement bar fracture due to longitudinal reinforcement bar buckling after spalling of concrete cover in the plastic hinge region. It is worth noting that spiral spacing was similar for all of the columns and that shear failures were precluded through capacity design during the experimental design;

5. The overstrength factor used to predict the column moment capacity in this paper for columns constructed with Grade 80 reinforcement were slightly lower than the computed overstrength factor used for columns constructed with Grade 60 reinforcement;
6. The effects of the longitudinal reinforcement ratio were similar between the columns constructed with Grade 60 reinforcement and the columns constructed with Grade 80 reinforcement. The columns constructed with Grade 60 reinforcement and the columns constructed with Grade 80 reinforcement exhibited a larger computed overstrength factor with an increase in the longitudinal reinforcement ratio.

The results in this study present a promising step towards the implementation of Grade 80 reinforcement in the design and construction of RC bridge columns, within the bounds of the variables used in the experimental program. Other parameters outside of the range studied in this paper should be evaluated such as larger longitudinal reinforcement ratios, larger axial load ratios, and higher concrete strengths. It should be noted that the design procedure for the use of Grade 80 reinforcement in other areas of AASHTO bridge design standards are not clear and additional research is needed.

2.7 REFERENCES

A01 Committee. 2013. “Test Methods and Definitions for Mechanical Testing of Steel Products”. ASTM International. http://enterprise.astm.org/filtrexx40.cgi?+REDLINE_PAGES/A370.htm.

ASTM. 2009. “A706/A706M-09b Standard Specification for Low-Alloy Deformed and Plain Bars for Concrete Reinforcement.”

C09 Committee. 2010. “Test Method for Flexural Strength of Concrete (Using Simple Beam with Third-Point Loading)”. ASTM International. http://enterprise.astm.org/filtrexx40.cgi?+REDLINE_PAGES/C78C78M.htm.

———. 2011. “Test Method for Splitting Tensile Strength of Cylindrical Concrete Specimens”. ASTM International. http://enterprise.astm.org/filtrexx40.cgi?+REDLINE_PAGES/C496C496M.htm.

———. 2012. “Practice for Making and Curing Concrete Test Specimens in the Field”. ASTM International. http://enterprise.astm.org/filtrexx40.cgi?+REDLINE_PAGES/C31C31M.htm.

———. 2014a. “Test Method for Compressive Strength of Cylindrical Concrete Specimens”. ASTM International. http://enterprise.astm.org/filtrexx40.cgi?+REDLINE_PAGES/C39C39M.htm.

———. 2014b. “Test Method for Static Modulus of Elasticity and Poissons Ratio of Concrete in Compression”. ASTM International. http://enterprise.astm.org/filtrexx40.cgi?+REDLINE_PAGES/C469C469M.htm.

Concrete Reinforcing Steel Institute. 2001. “Evaluation of Reinforcing Bars in Old Reinforced Concrete Structures”. Engineering Data Report 48.

E28 Committee. 2010. “Practice for Verification and Classification of Extensometer Systems”. ASTM International. http://enterprise.astm.org/filtrexx40.cgi?+REDLINE_PAGES/E83.htm.

———. 2013. “Test Methods for Tension Testing of Metallic Materials”. ASTM International. http://enterprise.astm.org/filtrexx40.cgi?+REDLINE_PAGES/E8E8M.htm.

Gustafson, David P. 2010. “Raising the Grade.” Concrete International 32 (04): 59–62.

Mander, J., F. Panthaki, and A. Kasalanati. 1994. “Low-Cycle Fatigue Behavior of Reinforcing Steel.” Journal of Materials in Civil Engineering 6 (4): 453–68. doi:10.1061/(ASCE)0899-1561(1994)6:4(453).

Priestley, M. J. N., and G. Benzoni. 1996. “Seismic Performance of Circular Columns with Low Longitudinal Reinforcement Ratios.” ACI Structural Journal 93 (4): 474–85.

Priestley, Michael John Nigel. 2003. Myths and Fallacies in Earthquake Engineering, Revisited. IUSS press.

Rautenberg, J.M., S. Pujol, and A. Lepage. 2010. “Cyclic Response of Concrete Columns Reinforced with High-Strength Steel.” 9th US National and 10th Canadian Conference on Earthquake Engineering 2010, Including Papers from the 4th International Tsunami Symposium 3 (July). http://nees.org/resources/679/download/2010EQConf-000996.PDF.

Rice, Pual, and David Gustafson. 1976. “Grade 80 Reinforcing Bars and ACI 318-71.” Journal Proceedings 73 (4): 199–206.

Risser, Robert, and Michael Hoffman. 2014. “Turning Billets into Bars.” Concrete Construction. Accessed May 29. http://www.concreteconstruction.net/rebar/turning-billets-into-bars.aspx.

Rodriguez, M., J. Botero, and J. Villa. 1999. “Cyclic Stress-Strain Behavior of Reinforcing Steel Including Effect of Buckling.” Journal of Structural Engineering 125 (6): 605–12. doi:10.1061/(ASCE)0733-9445(1999)125:6(605).

Trejo, David, Andre Barbosa, and Tim Link. 2014. “Seismic Performance of Circular Reinforced Concrete Bridge Columns Constructed with Grade 80 Reinforcement”. Research SRS 500-610. Oregon State University.

Yeh, I-Cheng. 2006. “Generalization of Strength versus Water–cementitious Ratio Relationship to Age.” Cement and Concrete Research 36 (10): 1865–73. doi:10.1016/j.cemconres.2006.05.013.

2.8 ACKNOWLEDGMENTS

The authors would first like to acknowledge ODOT and PacTrans for providing the funding for this research project. As with all projects, the success of the project is dependent on many dedicated people. We would like to thank Michael Dyson, James Batti, and Manfred Dittrich for their assistance in fabricating and testing the specimens. Students that assisted with the project include Jiaming Chen, Nicolas Matus, Greg Hendrix, Cody Tibbits, Lapyote Prasittisopin, Yicheng Long, Frank Porter, Amy Kordoska, and Drew Nielson. The assistance of Dana Ainsworth, our expert in all things financial, is duly noted. The assistance of Farwest Steel (Eugene, OR) for assisting with the fabrication of the reinforcement is greatly appreciated.

Special thanks to Thomas Murphy and Dennis Laubar from Cascade Steel (McMinnville, OR) for producing a special heat of Grade 80 reinforcement. The authors sincere thank all those that assisted with work developed in this study.

2.9 TABLES AND FIGURES

2.9.1 List of Tables:

Table 2.1 Experimental test matrix of columns G60-1, G80-1, G60-2 and G80-2.....29

Table 2.2 Loading profile of columns G60-1, G80-1, G60-2 and G80-2 29

Table 2.3 Columns G60-1, G80-1, G60-2 and G80-2 capacities..... 30

Table 2.4 Summary of ductility values of columns G60-1, G80-1, G60-2 and G80-2 30

Table 2.5 Energy dissipation of columns G60-1, G80-1, G60-2 and G80-2 30

2.9.2 List of Figures:

Figure 2.1 (a) Columns G60-1, G80-1, G60-2 and G80-2 cross-sections (b) test specimen geometry of G60-1, G80-1, G60-2 and G80-2 31

Figure 2.2 Columns G60-1, G80-1, G60-2 and G80-2 internal instrumentation.....31

Figure 2.3 Columns G60-1, G80-1, G60-2 and G80-2 external instrumentation (NTS = not to scale).....32

Figure 2.4 Loading profile of columns G60-1, G80-1, G60-2 and G80-2.....32

Figure 2.5 Photograph of column G80-1 crack mapping and concrete spalling.....33

Figure 2.6 Shear force versus drift ratio of columns: (a) G60-1 and G80-1, (b) G60-2 and G80-2.....33

Figure 2.7 Cumulative energy dissipation 34

Table 2.1 Experimental test matrix of columns G60-1, G80-1, G60-2 and G80-2

Specimen	Concrete strength	Longitudinal reinforcement
G60-1	4.77 ksi (32.9 MPa)	Grade 60 ksi (420 MPa) 16 #5 (#16M) ρ_l = 1.11%
G80-1	4.84 ksi (33.4 MPa)	Grade 80 ksi (550 MPa) 12 #5 (#16M) ρ_l = 0.83%*
G60-2	3.59 ksi (24.7 MPa)	Grade 60 ksi (420 MPa) 22 #6 (#19M) ρ_l = 2.19 %
G80-2	4.66 ksi* (32.1 MPa)*	Grade 80 ksi (550 MPa) 16 #6 (#19M) ρ_l = 1.58%

* Tested data is not available, Abram's Formula with experimental parameter equations determined by Yeh (2006) was used to estimate the concrete strength

Table 2.2 Loading profile of columns G60-1, G80-1, G60-2 and G80-2

Displacement cycle, in. (mm)	Number of cycles	Loading rate, in/s (mm/s)
0.10 (2.5)	3	0.01 (0.25)
0.25 (6.4)	3	0.01 (0.25)
0.50 (13)	3	0.01 (0.25)
0.75 (19)	3	0.01 (0.25)
1.00 (25.4)	3	0.01 (0.25)
1.25 (31.8)	3	0.02 (0.51)
2.50 (63.5)	3	0.04 (1.0)
3.75 (95.3)	3	0.08 (2.0)
5.00 (127)	3	0.08 (2.0)
6.25 (159)	3	0.08 (2.0)
7.50 (191)	3	0.08 (2.0)
8.75 (222)	3	0.08 (2.0)
10.00 (254)	3	0.16 (4.1)

Table 2.3 Columns G60-1, G80-1, G60-2 and G80-2 capacities

Specimen	Maximum applied force kip (kN)	Maximum shear force kip (kN)	Associated plastic shear kip (kN)	Nominal moment capacity (Response 2000)	Tested moment capacity kip-ft (kN-m)	Expected moment capacity kip-ft (kN-m)	Computed overstrength factor, λ
G60-1	28.9 (128.4)	25.9 (115.1)	33.58 (149.4)	288 (390)	354 (480)	403 (546)	1.23
G80-1	28.2 (125.6)	25.9 (115.1)	33.22 (147.8)	285 (386)	344 (466)	399 (541)	1.21
G60-2	52.0 (231)	47.9 (213)	54.0 (240)	463 (628)	631 (856)	649 (880)	1.36
G80-2	46.9 (209)	43.1 (192)	52.3 (233)	448 (607)	572 (776)	628 (851)	1.28

Table 2.4 Summary of ductility values of columns G60-1, G80-1, G60-2 and G80-2

Specimen	Displacement ductility, μΔ		Curvature ductility, μψ				
	Reference yield	First yield	Level 1	Level 2	Level 3	Level 4	Level 5
G60-1	3.95	5.83	20.34	8.54	3.54	0.93	0.69
G80-1	4.13	5.51	16.45	9.66	2.38	1.19	0.63
G60-2	4.58	7.00	20.89	19.16*	6.63	2.32	0.84
G80-2	4.35	6.33	23.63	10.21	5.61	1.54	1.43

*Note this large value is believed to have occurred due to the excessive deep spalling on the south side of the column reducing the compressive resistance of the column resulting in larger curvature in this region. It should also be noted this value occurred on the final peak of the 10.00-inch (254mm) displacement cycle shortly prior to column failure.

Table 2.5 Energy dissipation of columns G60-1, G80-1, G60-2 and G80-2

	G60-1	G80-1	G60-2	G80-2
Energy dissipated at first yield, kip-ft (kN-m)	3.24 (4.39)	4.78 (6.48)	6.43 (8.72)	5.97 (8.09)
Energy dissipated at reference yield, kip-ft (kN-m)	5.48 (7.43)	5.80 (7.86)	9.01 (12.2)	8.07 (10.9)
Total energy dissipated at column failure, kip-ft (kN-m)	193.48 (262.32)	150.33 (203.82)	684.24 (927.71)	457.67 (620.52)

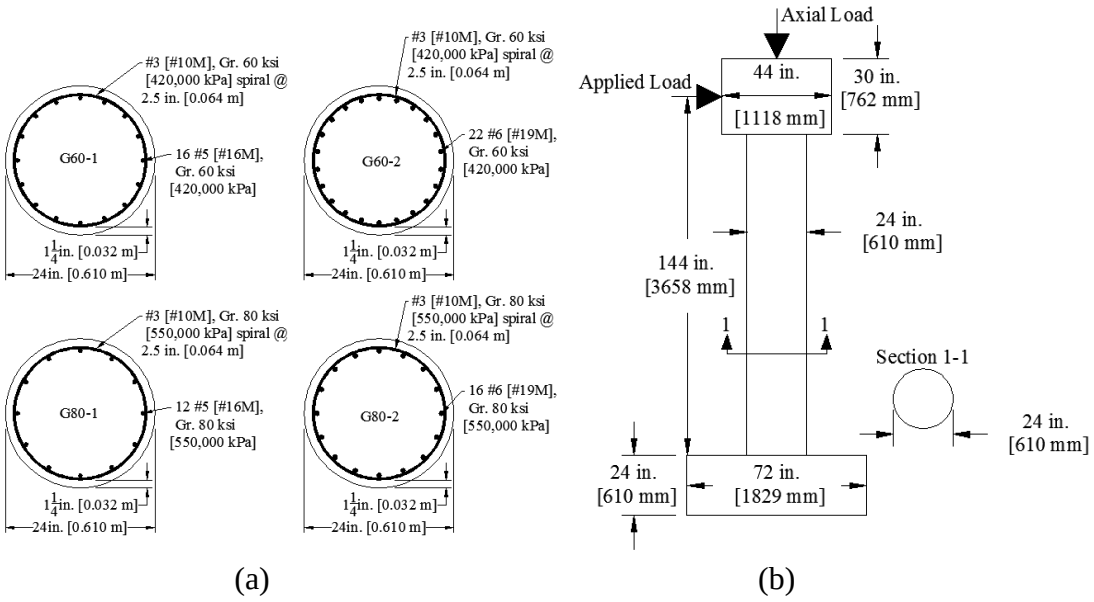

Figure 2.1 (a) Columns G60-1, G80-1, G60-2 and G80-2 cross-sections (b) test specimen geometry of G60-1, G80-1, G60-2 and G80-2

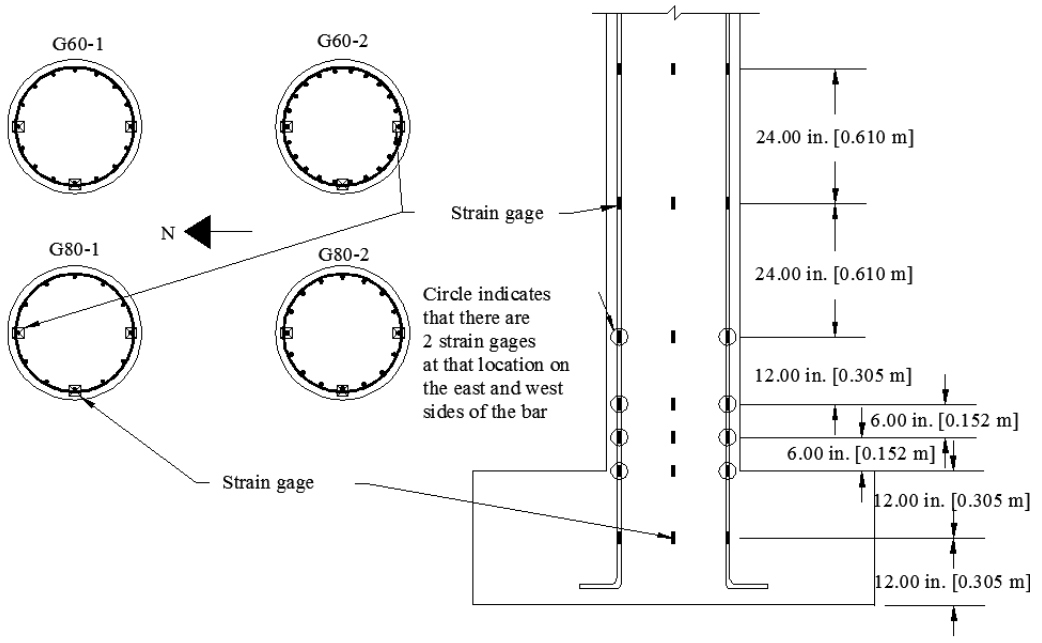

Figure 2.2 Columns G60-1, G80-1, G60-2 and G80-2 internal instrumentation

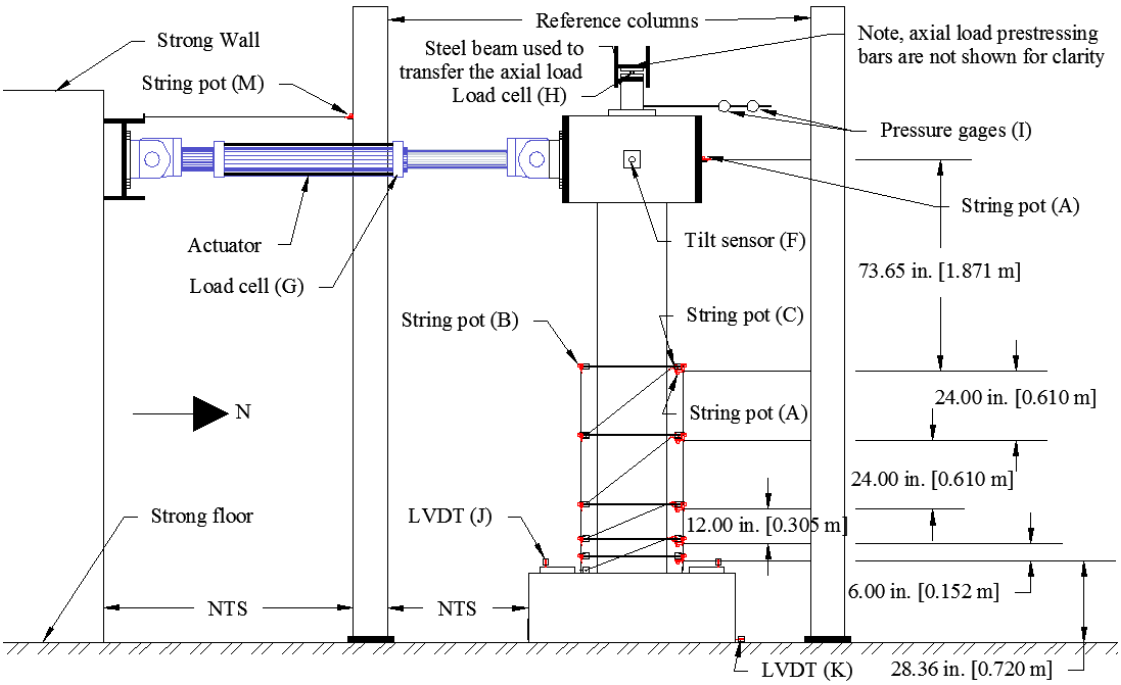

Figure 2.3 Columns G60-1, G80-1, G60-2 and G80-2 external instrumentation (NTS = not to scale)

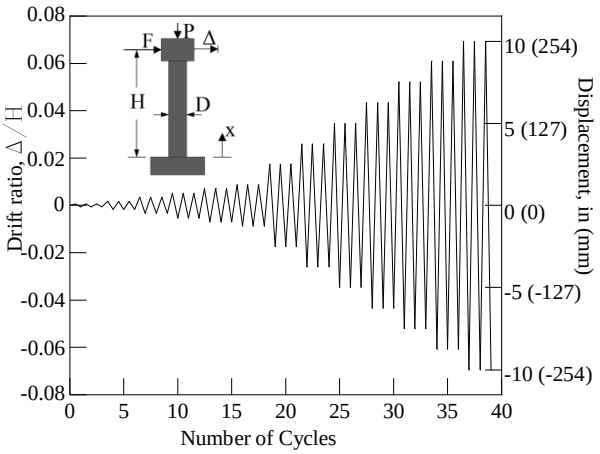

Figure 2.4 Loading profile of columns G60-1, G80-1, G60-2 and G80-2

Figure 2.5 Photograph of column G80-1 crack mapping and concrete spalling

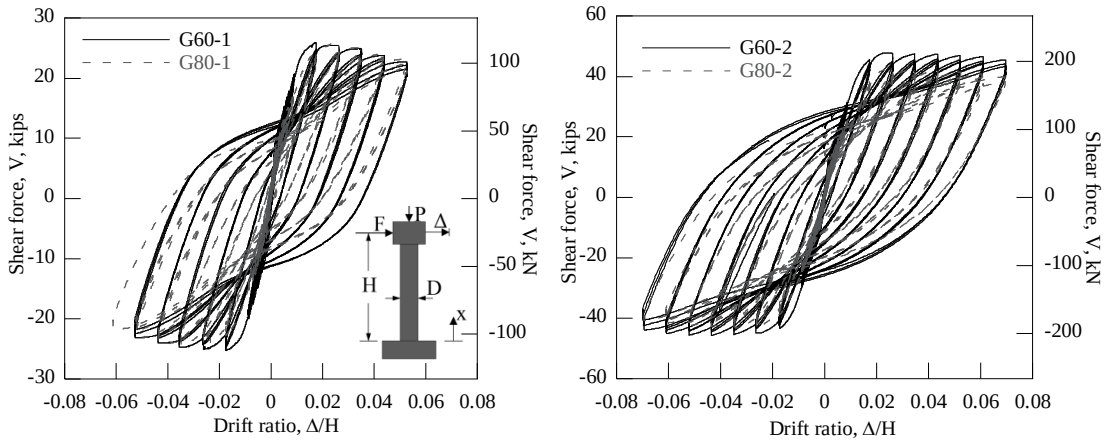

(a) (b)

Figure 2.6 Shear force versus drift ratio of columns: (a) G60-1 and G80-1, (b) G60-2 and G80-2

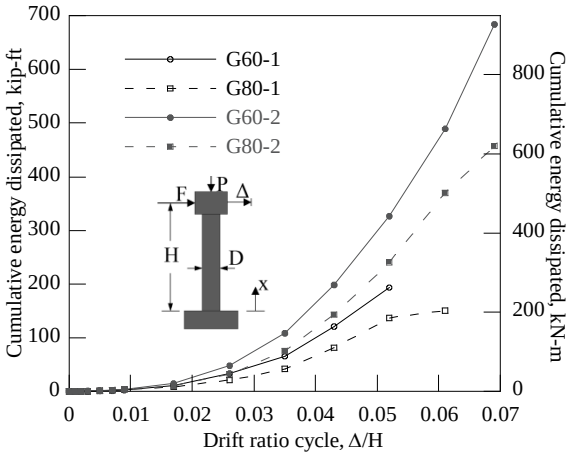

Figure 2.7 Cumulative energy dissipation

Chapter 3 SEISMIC PERFORMANCE OF HIGH STRENGTH STEEL RC BRIDGE COLUMNS

Will be submitted to:

Journal of Bridge Engineering (ASCE)

American Society of Civil Engineers

1801 Alexander Bell Drive

Reston, VA 20191

3.1 ABSTRACT

The American Society for Testing and Materials (ASTM 2009) currently has a specification for low alloy reinforcing steel with a nominal yield stress of 80 ksi (550 MPa). However, the American Association of State Highway and Transportation Officials (AASHTO) and specifications for select State Highway Agencies (SHAs) do not allow the use of Grade 80 reinforcement in structural concrete members designed to form a bending moment plastic hinge. This limitation is due to lack of information on the material characteristics of ASTM A706 Grade 80 reinforcement and loack of test data on the cyclic performance of plastic hinges in compression members. The use of Grade 80 reinforcement could improve constructability, increase structural performance, and/or reduce material quantities. This research investigated the performance of circular concrete bridge columns constructed with Grade 80 reinforcement. Two pairs of columns were tested (four columns in total). Each pair consisted of one column constructed with Grade 80 reinforcement and the other column constructed with Grade 60 reinforcement. Each pair of columns were designed to have similar moment capacities. The first pair had a moment-shear span ratio of six while the second pair had a moment-shear span ratio of three. The columns were subjected to lateral cyclic loading to determine the effects of the steel reinforcement grade and the effect of the moment-shear span ratio on column performance. Results indicate that the columns constructed with Grade 80 reinforcement achieved similar resistance, similar maximum lateral displacements, and similar displacement ductility values when compared with the reference columns constructed with Grade 60

reinforcement. However, columns constructed with Grade 80 reinforcement exhibited lower hysteretic energy dissipation compared to the columns constructed with Grade 60 reinforcement. Results also indicate that the effect of the moment-shear span ratio on column performance is similar for columns constructed with either Grade 60 or Grade 80 reinforcement.

Keywords: ASTM A706 Grade 80; circular columns; cyclic tests; high-strength steel reinforcement; moment-shear span ratio; reinforced concrete bridge columns; seismic performance

3.2 INTRODUCTION

In 2012, AASHTO and SHAs allowed the use of Grade 80 reinforcement, but have restricted the use in members designed to form a plastic moment hinge such as bridge columns in seismic regions. In seismic regions, reinforcement congestion can present a significant challenge (Gustafson 2010; Risser and Hoffman 2014). The lack of experimental data on columns constructed with Grade 80 rienforcement has limited the use of this type of high strength steel (HSS) reinforcement in bridge columns. The primary reason for limiting the use of Grade 80 reinforcement is because increasing yield strength typically results in decreased strain ductility. In addition, designers are reluctant to specify Grade 80 reinforcement because it can currently only be used in certain structural members and potential errors in placement could arise; i.e., placing Grade 60 reinforcement where Grade 80 reinforcement is required or vice versa.

The main objective of this study is to provide experimental data on the lateral cyclic performance of bridge columns constructed with Grade 80 reinforcement. In this study, an experimental plan was developed to assess the effects of reinforcement grade (yield strength) and the moment-shear span ratio on column performance. Ultimately, the main outcome of this study is to provide seminal data to support SHAs in their design of bridges constructed with Grade 80 reinforcement.

A review on the evolution of reinforcement grade can provide information on why Grade 80 reinforcement is not used in RC bridge columns in the US, even though similar strength steel reinforcements are currently used in other countries with similar seismic challenges. The first concrete reinforcement specification in the US was developed by the American Association of Steel Manufacturers in 1910 (Concrete Reinforcing Steel Institute 2001). Shortly after, ASTM adopted the standard specification A15 for billet steel reinforcement, which had a structural yield strength of 33,000 psi (228 MPa). This standard was in place for many years. It was only in 1959, that ASTM developed specifications for concrete reinforcement with yield strengths of 60 ksi (414 MPa) and 75 ksi (520 MPa) (Gustafson 2010). According to Gustafson (2010), in 1967 engineers began recognizing the potential benefits of HSS reinforcement and reports identified that Grade 80 reinforcement could be economically used and produced and would be in demand if produced.

Following the 1967 reports, Rice and Gustafson (1976) analytically assessed the moment capacity of structural elements constructed with Grade 80 reinforcement.

Through the use of moment interaction diagrams the authors showed that columns constructed with Grade 80 reinforcement exhibited a significant increase in moment capacity compared to columns constructed with Grade 60 reinforcement. An economic analysis was also performed by the authors and they reported that the use of Grade 80 reinforcement could have a significant reduction in cost if large quantities were manufactured.

Even with the potential benefits of HSS reinforcement identified almost 40 years ago, limited research has been performed on the cyclic performance on the material The research on the seismic performance of columns constructed with HSS reinforcemen has been limited. Rautenberg et al. (2010) reported that HSS reinforcement can reduce bar congestion without significantly reducing the performance for RC columns with low axial loads. Test results indicated that columns constructed with Grade 60 (ASTM A615) and Grade 120 (ASTM A1035) reinforcement both exhibited drift ratios exceeding 4 percent and both had similar moment capacities. The authors reported that as long as the fracture strain of the longitudinal reinforcement exceeds seven percent for a reference gage length of eight inches (203 mm) and the amount and detailing of the transverse reinforcement is adequate to prevent shear failure, bond failure, and bar buckling, then the amount of reinforcement can be reduced proportionally with the increased yield strength. The authors also reported a noticeable reduction in hysteretic energy dissipation between the columns constructed with Grade 60 reinforcement and the columns constructed with Grade 120 reinforcement. However, the authors noted that the difference was a result of the difference in column stiffness, the column

constructed with the Grade 120 reinforcement had approximately half the amount of longitudinal reinforcement as the columns constructed with Grade 60 reinforcement. Due to this, the columns constructed with Grade 120 reinforcement had approximately half the stiffness as the columns constructed with Grade 60 reinforcement. Columns constructed with Grade 80 reinforcement will likely exhibit a decrease in hysteretic energy dissipation compared to columns constructed with Grade 60 reinforcement design to have the same moment capacity, but testing is needed to addres this claim.

Limited tests have been performed using Grade 80 reinforcement and thus there is a lack of testing on the effect of the moment-shear span ratio (Berry and Eberhard 2008). Lehman et al. (2004) evaluated the seismic performance of ten RC columns with four different aspect ratios. Although the columns were constructed with Grade 60 reinforcement the test column dimensions, material properties and loading procedure are similar to some of the columns presented in this paper. Lehman et al. (2004) experimental results indicated that as the aspect ratio increased the yield displacement increased, the displacement when initial spalling occurred increased, and the displacement cycle when bar buckling and bar fracture occurred also increased. Additionally, Lehman et al. (2004) test results indicated that as the aspect ratio increased the maximum lateral displacement increased and the lateral force capacity decreased. Li et al. (2014) and Pham and Li (2014) also reported that a decrease in the aspect ratio increased the lateral strength and that the decrease in aspect ratio also decreased the maximum lateral displacement of the columns.

Potential benefits of using Grade 80 reinforcement exist, however significant questions still remain. The main goal of this paper is to answer some of those questions throught the comparison of the experimental behavior of four RC columns. The extent to which strain ductility of the material is important in defining the displacement and curvature ductilities of the columns is also unknown. The affect on energy dissipation of RC systems containing Grade 80 reinforcement is not well defined. The effects of the moment-shear span ratio (aspect ratio) on columns constructed with Grade 80 reinforcement will also be assessed and quantified in this paper by reporting experimental results obtained for two different moment-shear span ratios.

This research is important since lower quantities of reinforcement and reduced congestion can be achieved by using Grade 80 reinforcement in RC bridge columns if research results can show similar and safe performance of the columns subjected to layeral cyclic loading. In this study, testing was performed on four half-scale circular RC bridge columns. Two pairs of columns were tested and evaluated to determine the effects of reinforcement grade and the effect of the moment-shear span ratio. The results can be used to assess the potential use of Grade 80 reinforcement in RC bridge columns subjected to seismic loads.

3.3 EXPERIMENTAL PLAN AND PROCEDURE

An experimental plan was developed to assess the seismic performance of RC bridge columns constructed with ASTM A706 Grade 80 reinforcement when subjected to

lateral cyclic loading. The experimental plan consisted of testing two pairs (4 columns in total) of half-scale columns. Two columns were constructed with Grade 60 reinforcement and the other two columns were constucted with Grade 80 reinforcement, both grades meet ASTM A706 specifications. The experimental plan is shown in Table 3.1. The first pair of columns, G60 and G80, are representative of a bridge containing a single pier loaded in the transverse direction. The second pair of columns, G60-s and G80-s, are representative of a bridge pier loaded in the longitudinal direction. The first pair of columns, G60 and G80, have a moment-shear span ratio equal to six. The second pair of columns, G60-s and G80-s, have a moment-shear span ratio equal to three. The “G60” represents columns constructed with Grade 60 reinforcement, the “G80” represents columns constructed with Grade 80 reinforcement, and the“s” represents the shorter columns.

3.3.1 Test Specimen Design

Columns G60 and G60-s were designed with a longitudinal reinforcement ratio of 2.19 percent corresponding to 22 #6 (22 ø19 mm) Grade 60 reinforcement bars. Columns G80 and G80-s were designed to provide approximately the same moment capacity as columns G60 and G60-s but were constructed with Grade 80 reinforcement rather than Grade 60 reinforcement. Columns G80 and G80-s have a longitudinal reinforcement ratio of 1.58 percent corresponding to 16 #6 (16 ø19 mm) Grade 80 reinforcement bars. Note that the increase in the ratio of nominal yield strength did not perfrectly math the decreae in the ratio of the number of longitudinal reinforcemen bars. The increae in nominal yiled strength ratio was 1.33 and the decrease in the number of

longitudinal bars was 1.38. Additional details on the specimen design can be found in the research report by Trejo et al. (2014).

Figure 3.1 shows the cross-sectionsand column dimensions. The column test height, H, is equal to 12 feet (3.66 m) for the first pair of columns (G60 and G80) and is equal to 6 feet (1.83 m) for the second pair of columns (G60-s and G80-s). All columns tested were 2-feet (0.61 m) in diameter, which correspound to half-scale speciments of a typical 4-feet (1.22 m) diameter column built in the Western US, including California, Oregon, and Washington. The total weight, including the Rc load stub and footing was was 10.45 (short-U.S.) tons (9.48 metric tonnes) for the taller columns and was was 9.04 (short-U.S.) tons (8.20 metric tonnes) for the shorter columns.

All four columns had a nominal concrete compressive strength of 4000 psi (27.6 MPa). Table 3.1 shows the tested concrete compressive strength at the day of testing for each column. It should be noted that the difference in concrete strengths is primarily due to the age of the concrete at the time of testing. It should also be noted that the difference in concrete strength only has a small effect on the performance of the columns. All four columns have the same spiral pitch (spacing) of 2.50 inches (63.5 mm). The spiral reinforcement bar size is #3 (#10M) for all columns. The pitch and bar size corresponds to a transverse reinforcement ratio of 0.82 percent. The transverse reinforcement ratio, ρ_t, was computed as the ratio of the volume of the spiral reinforcement to the volume of the core. The longitudinal reinforcement ratio, ρ_l, was computed as the cross-sectional area of longitudinal reinforcement steel

divided by the gross area of the column minus the cross sectional area of longitudinal reinforcement.

3.3.2 Construction Sequence

Concrete casting was done in two pours for each pair of columns, which were cast with the same batch of concrete on the same day to reduce variability in the material. First, the fotting was cast, and then the columns and load load stubs were cast a week later. Columns G60 and G80 were cast on the same day and columns G60-s and G80-s were cast on the same day. The concrete mixture contain a ⅜-inch (9.5 mm) maximum size aggregate (MSA). The concrete mixture was also proportioned to be pumpable and had a minium required slump of 5 inches (127 mm). The reported concrete unit weight was 142 lb/ft^3 (22.5 kN/m^3).

3.3.3 Instrumentation

Each test column was instrumented to quantify indicators of column performance during cyclic testing. A total of 29 strain gages were placed on both the longitudinal (22 strain gages) and transverse (7 strain gages) reinforcement for columns G60 and G80 as shown in Figure 3.2. Columns G60-s and G80-s have two fewer longitudinal strain gages and one less transverse strain gage compared to columns G60 and G80. Strain gages on the longitudinal reinforcement were placed on the outer edges perpendicular to the direction of the applied horizontal load. Two strain gages each were placed on the longitudinal reinforcement within the region whre significant inelastic strains were expect to develop (24 inches [610 mm]). Single strain gages

were placed outside of the plastic hinge region. Strain gages on the transverse reinforcement (spiral) were placed on the outer most surface of the spiral at approximately the same elevations as the strain gages on the longitudinal reinforcement. Figure 3.2 shows the locations of the strain gages in columns G60-s and G80-s are shown in. The lowest elevation is referred to as level 1 and the highest elevation is referred to as level 6. Note that columns G60 and G80 had strain gages at the same locations as columns G60-s and G80-s up to level 5. Two ⅜-inch (9.5 mm) diameter threaded rods were cast with the concrete column at four different elevations (two rods each at the four levels; eight rods in total). The rods were spaced at either four inches (102 mm) or five inches (127 mm) horizontally and were centered in the column. The 4-inch (102 mm) spacing was the default spacing and the 5-inch (127 mm) spacing was used when the longitudinal reinforcement prevented the default spacing from being used. Aluminum angles were attached to the threaded rods. Sixteen string potentiometers, label B, (two on each aluminum angle) were attached to the aluminum angles to obtain measurements to determine the column curvatures. Figure 3.3 shows the locations of the string potentiometers and additional instrumentation for columns G60-s and G80-s are shown in. Note that the locations of the bottom three levels are identical for columns G60 and G80. A load cell within the actuator, label G, was used to measure the applied horizontal load and one string potentiometer, label A, was used to measure the tip displacement. Details on additional instrumentation can be found Trejo et al. (2014).

3.3.4 Test Setup and Testing Procedure

Test set-up initiated with stressing the column footing to the strong floor. For the second pair of columns (G60-s and G80-s) a RC spacer block was placed between the bottom of the column footing and the strong floor. The hydraulic actuator was then bolted to the RC header and the axial load system was assembled. The axial load was applied with a hydraulic jack located between the top of the load stub (header) and a steel reaction beam. The steel reaction beam (6-feet [1.83 m] W12x152) was connected to the column footing using prestressing threaded rods. The initialapplied axial load was 90 kips (400 kN), corresponding to five percent of the nominal axial capacity of the column in compression. The test setup included a system to minimize fluctiontaions in the axial load.

Table 3.2 shows the displacement testing protocol and Figure 3.4 shows the profile in terms of drift ratio versus the number of cycles. Horizontal loading consisted of pushing and pulling the column (in the north-south direction) to predetermined drift ratio levels. Each drift ratio level consisted of three cycles (six peaks): each cycle started at zero displacement, was then displaced in the positive direction towards the positive peak (North), was then displaced in the negative direction towards the negative peak (South), and was then returned back to zero displacement. This process was repeated three times for each predetermined drift ratio level. Both pairs of columns were tested at the same drift ratio levels. Thus, to achieve the same drift ratios the tip displacements of the second pair of columns (G60-s and G80-s) were half the value of the tip displacements of the first pair of columns (G60 and G80).

To characterize the material properties of the concrete and steel reinforcement used, several material tests were performed. Concrete material testing included: compressive strength tests ((ASTM C39) C09 Committee 2014a), splitting tensile strength tests ((ASTM C496) C09 Committee 2011), modulus-of-elasticity tests ((ASTM C469) C09 Committee 2014b), and modulus-of-rupture tests ((ASTM C78) C09 Committee 2010) were performed. Concrete samples were made and cured following ASTM C31 specifications (C09 Committee 2012). The reinforcement strength and strain parameters were obtained from tension tests performed using a 110-kip universal testing machine following ASTM E8 (E28 Committee 2013), E83 (E28 Committee 2010) and A370 (A01 Committee 2013) specifications.

3.4 TEST RESULTS AND ANALYSIS

The two pairs of columns (G60 and G80, G60-s and G80-s) were compared to determine the effects of the steel reinforcement grade and the effect of moment-shear span ratio on the column performance. Steel reinforcement strains, column capacity, column ductility, and energy dissipation are compared in this paper. All four columns exhibited a flexure failure. Longitudinal reinforcement bar buckling followed by longitudinal reinforcement bar fracture was the mode of failure for all of the columns.

3.4.1 Steel Reinforcement Strains

The longitudinal reinforcement in columns G60-s and C80-s yielded during the 0.7 percent drift ratio cycle. The longitudinal reinforcement in column G60-s initially yielded at a tip displacement of -0.50 inches (-13 mm) at 12 inches (305 mm) from the

base of the column (level 4), which corresponds to a drift ratio of 0.69 percent. The longitudinal reinforcement in column G80-s initially yielded at a tip displacement of -0.56 inches (-14 mm) at 6 inches (152 mm) from the base of the column (level 3), which corresponds to a rift ratio of 0.78 percent.

The longitudinal reinforcement in column G60 initially yielded at a tip displacement of 1.44 inches (36.6 mm), which corresponds to a drift ratio of 1.00 percent. This occurred during the approach to the first peak of the 1.7 percent drift ratio cycle at the base of the column (level 2). The data indicates that a decrease in the moment-shear span ratio of columns constructed with Grade 60 reinforcement may cause the longitudinal reinforcing bars to yield earlier. At level 2, the longitudinal reinforcement in column G80 initially yielded during the 1.7 percent drift ratio cycle. When comparing columns G80-s and G80, column G80 was able to complete two more drift ratio cycles prior to the longitudinal reinforcement yielding. This result was similar to the difference between columns G60 and G60-s. This indicates that a decrease in the moment-shear span ratio causes the longitudinal reinforcing bars to yield earlier for columns constructed with either Grade 60 or Grade 80 reinforcement.

At strain gage level 1 (inside the footing), column G60 initially yielded on the 2.6 percent drift ratio cycle while column G60-s instility yieldon the on the 1.7 percent drift ratio cycle. The longitudinal reinforcement in column G80-s yielded during the 0.7 percent drift ratio cycle and the longitudinal reinforcing bars in column G80 never yielded in the footing (level 1). The level at which the maximum strains develop for

the columns constructed with Grade 80 reinforcement when compared to the columns constructed with Grade 60 reinforcement indicate that the strain penetration effects are larger in the columns constructed with Grade 60 reinforcement. The strain penetration can be estimated by integrating the tension reinforcement strain profile below the base of the column and the fact that the strain in the bars are lower for the columns constructed with Grade 80 reinforcement indicate that the strain penetration is smaller. The length of the strain penetration is a function of the yield strength of the longitudinal reinforcement, therefore it would be expected that the effects of strain penetration would be larger for the columns reinforcement with Grade 80 reinforcement, however this is not what the experimental data exhbits. A possible explantation of this would be the fact that the Grade 80 reinforcement has a larger development length. The experimental data consistently shows that the columns constructed with Grade 80 reinforcement exhibited the maximum strains in the longitudinal reinforcement further above the base of the column compared to the columns constructed with Grade 60 reinforcement.

3.4.2 Column Capacity

In this section, column capacities discussed include: maximum column shear force, tested moment capacity, and computed overstrength factor. Table 3.3 shows column capacities and overstrength factors. It is worth nothing that calculations were performed to eliminate the geometry effects of the applied axial load.

Figure 3.5 shows the shear force versus drift ratio of columns G60-s and G80-s up to the first longitudinal reinforcement fracture. It can be seen that there are slight differences in the peak strength capacity. The difference in the maximum shear force was expected because the nominal moment capacities of the columns were different due to the fact that the increase in yield strength of the longitudinal reinforcement was not perfectly proportional to the reduction in the area of the longitudinal reinforcement. Table 3.3 reports the maximum test shear force and test moment capacity. The computed overstrength factor, defined as the ratio of the test moment capacity to the nominal moment capacity is shown in Table 3.3. For column G60-s the computed overstrength factor of 1.36 is obtained and for column G80-s the computed overstrength factor of 1.28 is obtained. The lower value of the computed overstrength factor may indicate that the value should be reduced when columns are constructed with Grade 80 reinforcement.

It can be seen that the overall shape of the hysteretic loops are similar, but column G60-s exhibited a slightly larger shear force and considerably greater energy dissipation

Columns G60 and G60-s and columns G80 and G80-s have a computed overstrength values of 1.36 and 1.28, respectively. This suggests that the moment-shear span ratio does not affect the computed overstrength factor. As shown in Table 3.3 the overstrength factor obtained by following the AASHTO Guide Specifications LRFD Seismic Bridge Design (2011) procedure is smaller than the computed overstrength

factor for all of the columns. The AASHTO overstrength factor is the ratio of the plastic moment capacity to the nominal moment capacity. The plastic moment capacity was determined using Response-2000 with a concrete resistance factor of 1.3 and and the reinforcement resistance factor of 1.2.

Figure 3.6(a) and 3.6(b) show the shear force versus drift ratio up to the first longitudinal reinforcement fracture of columns G60 and G60-s and columns G80 and G80-s, respectively. These figures indicate the shorter columns (G60-s and G80-s) shear force are approximately twice the shear force of the taller columns (G60 and G80), as expected due to the shorter columns having half the moment-shear span ratio of the taller columns. However, the taller columns (G60 and G80) exhibited larger drift ratios prior to failure when compared to the shorter columns (G60-s and G80-s).

It should be noted that all four columns were very well detailed for confinement and shear forces were not expected to cause column failure, even for the relatively short columns with a moment-shear span ratio of 3. However, the result may not be extended to columns with larger reinforcement ratios as undesired compression failure of the core may govern the performance at failure. Future testing of columns with larger reinforcement ratios (i.e., above two percent) is needed to verfity this.

3.4.3 Column Ductility

Column ductility is defined in both displacement ductility and curvature ductility.

Table 3.4 provides a summary of the displacement and curvature ductility values. The displacement ductility is computed as the ratio of the maximum tip displacement to the

tip displacement at a reference yield point of the column. The reference yield point of the column is defined herein as the point when the longitudinal reinforcement reached a strain of one percent. This value was selected since it was observed in the material testing that for both Grade 60 and Grade 80 reinforcement strain hardening initiated at approximately one percent strain. The displacement ductility was also computed using the first yield displacement of the column longitudinal reinforcement as define previously. The curvature ductility is computed as the ratio of the maximum curvature and the reference yield curvature. The reference yield curvature ϕ_y was defined by Priestley (2003) for circular columns and is given by:

$$\phi_y = \frac{2.25\varepsilon_y}{D} \tag{3.1}$$

where ε_y is the yield strain of the longitudinal reinforcement and D is the column diameter. The flexural deformations of the column were obtained from vertical string potentiomers on either side of the column. The rotation at each instrumentation level was determined by taking the difference from the change in the North vertical string potentiometers and the change in the South vertical string potentiometers divided by the horizontal distance between the North and South vertical string potentiometers at each curvature instrumentation level. The rotation was divided by the vertical distance between each curvature instrumentation level to obtain the average curvature.

Three curvature instrumentation levels are used to study the effects of the moment-shear span ratio on the column curvature ductility.

The displacement ductility values based on the reference yield critiea are similar for columns G60-s and G80-s. However, when using the first yield criteria, the displacement ductility is larger for column G60-s when compared to column G80-s. Column G60-s exhibited significantly larger curvature ductility values at the curvature instrumentation levels 1, 3 and 4 when compared to column G80-s. However, column G80-s exhibited a significantly larger curvature ductility value at curvature instrumentation level 2 (12 inches [305mm] above the base of the column) when compared to column G60-s. The curvature ductility is typically more critical towards the base of the column where the majority of the curvature occurs. In this case, the data indicates that the curvature ductility value of column G60-s is greater than column G80-s at the base of the column (level 1) where strain penetration effects also influence the value. However, at level 2 where strain penetration effects do not affect the curvature ductility value, column G80-s exhibited larger curvature ductility values when compared to column G60-s, which can also be explained to the larger development length of the Grade 80 reinforcement.

Columns G60-s and G80-s exhibited larger displacement ductility values when using the reference yield and first yield criteria compared to column G60 and G80, respectivley. This suggests the decrease in moment-shear span ratio results in larger displacement ductility values. Columns G60-s and G80-s exhibited larger curvature ductility values towards the base of the column (level 1) compared to columns G60 and G80, respectively. However, for curvature ductility values not influenced by strain

penetration effects (levels 2 and 3) the decrease in the moment-shear span ratio decreases the curvature ductility values.

3.4.4 Energy Dissipation

The energy dissipated by each column was determined by numerical integration using the Simpson rule on the applied force over displacement hysteretic loops for each displacement cycle.

The hystertic energy dissipated, E_h ,is given by:

$$E_h = \int F(u)du \tag{3.2}$$

where F is the applied horizontal actuator force and u is the displacement measured by the horizontal string potentiometer at the same elevation as the applied horizontal actuator force.

It should be noted that energy dissipation is not a primary parameter used in design and most codes do not require a minimum value. Nonetheless, results are presented herin since energy dissipation becomes an important parameter when predicting the performance of structures and also when modeling structures to collapse.

Table 3.5 provides a summary of the energy dissipated at first yield and reference yield of the column, as well as the total energy dissipated up to the first reinforcement fracture for the four columns. Figure 3.7 shows the cumulative energy dissipated up to the first reinforcing bar fracture for the four columns.

Columns constructed with Grade 60 reinforcement (G60 and G60-s) exhibited greater energy dissipation between the first yield of the column and column failure when compared with the columns constructed with Grade 80 reinforcement (G80 and G80-s). This is likely a result of the reduction in the area of reinforcement in the columns constructed with Grade 80 reinforcement, which results in lower column stiffness. This in turn lowers its energy dissipation capacity. The energy dissipated at the first yielding of the longitudinal reinforcement of columns G60-s and G80-s were very similar.

The shorter columns (G60-s and G80-s) exhibited greater energy dissipation when compared with the taller columns (G60 and G80) prior to the failure drift ratio cycle. This is due to the increase in column stiffness of the shorter columns which resulted in a greater area within the hysteretic loops.

This indicates that a reduction in the moment-shear span ratio results in an increase in energy dissipation capacity after the longitudinal reinforcement has yielded for columns constructed with either Grade 60 or Grade 80 reinforcement mainly due to the increase in column stiffness. However, it should be noted that the columns with a larger moment-shear span ratio (columns G60 and G80) exhibited larger drift ratios prior to failure. This resulted in an overall increase in energy dissipation capacity at column failure when compared with columns with a smaller moment-shear span ratio (columns G60-s and G80-s).

3.5 SUMMARY AND CONCLUSIONS

The use of Grade 80 reinforcement in RC bridge columns has the potential to reduce reinforcement quantities, reduce reinforcement congestion, and improve the constructability, thus making the construction of new bridges more economical. However, limited research has been performed to validate the use of Grade 80 reinforcement, expecially in compression members that my develop plastic hinges. The research presented assessed the performance of two pairs columns through lateral cyclic testing. Each pair consisting of one column constructed with Grade 60 reinforcement and the other constructed with Grade 80 reinforcement. Both pairs of columns were designed to have similar moment capacities, but they had different moment-shear span ratios. Columns constructed with Grade 80 reinforcement were designed to achive the same moment capacity as the columns constructed with Grade 60 reinforcement. This was achieved by reducing the number of longitudinal reinforcement bars proportionally to the increase in nominal yield strength.

The main conclusions that can be drawn from these test results are:

1. Columns constructed with Grade 80 reinforcement achieved similar resistances when compared with the reference columns constructed with Grade 60 reinforcement. Note that the columns constructed with Grade 80 reinforcement had approximately ¾ the amount of longitudinal reinforcement of the columns constructed with Grade 60 reinforcement;

2. All four columns failed due to longitudinal reinforcement bar buckling followed by longitudinal reinforcement bar fracture. This indicates the mode of failure was flexural, however it should be noted that all of the columns were very well confined to prevent shear failure and other undesired modes of brittle failure;
3. Columns constructed with Grade 60 reinforcement and Grade 80 reinforced exhibited similar displacement ductility values when using the reference yield criteria. However, when using the first yield criteria the columns constructed with Grade 60 reinforcement exhibited larger displacement values compared to columns constructed with Grade 80 reinforcement;
4. Columns constructed with Grade 60 reinforcement typically exhibited larger curvature ductility values;
5. Columns constructed with Grade 80 reinforcement exhibited longer longituindal reinforcement development lengths and therefore exhibited smaller strain penetration effects;
6. The columns constructed with Grade 60 reinforcement exhibited larger hysteretic energy dissipation than the columns constructed with Grade 80 reinforcement. However, energy dissipation is primarily a function of the amount of longitudinal reinforcement and column stiffness rather than a function of the reinforcement grade;

7. Columns constructed with Grade 80 reinforcement tested in this research exhibited a computed overstrength factor slightly lower than the computed overstrength factor used for columns constructed with Grade 60 reinforcement;
8. The reduction in the moment-shear span ratio did not effect the computed overstrength factor for columns constructed with either grade of reinforcement;
9. The effects of the moment-shear span ratio were similar for columns constructed with Grade 60 reinforcement and columns constructed with Grade 80 reinforcement. The decrease in the moment-shear span ratio resulted in larger curvature ductility values at the base of the column where the effects of strain penetration affects the curvature and smaller curvature ductility values at higher elevations where the effects of strain penetration do not affect the curvature.

The results in this study present a promising step towards implementation of Grade 80 reinforcement in the design and construction of RC columns, within the bounds of the variables used in is testing program. Other parameters outside of the range studied in this paper should be evaluated. Those could include larger longitudinal reinforcement ratios and higher concrete strengths.

3.6 REFERENCES

A01 Committee. 2013. “Test Methods and Definitions for Mechanical Testing of Steel Products”. ASTM International. http://enterprise.astm.org/filtrexx40.cgi?+REDLINE_PAGES/A370.htm.

ASTM. 2009. “A706/A706M-09b Standard Specification for Low-Alloy Deformed and Plain Bars for Concrete Reinforcement.”

Berry, Michael P., and Marc O. Eberhard. 2008. “Performance Modeling Strategies for Modern Reinforced Concrete Bridge Columns”. PEER Report 2007/07. Pacific Earthquake Engineering Research Center. http://peer.berkeley.edu/publications/peer_reports/reports_2007/web_PEER707_BERRYeberhard.pdf.

C09 Committee. 2010. “Test Method for Flexural Strength of Concrete (Using Simple Beam with Third-Point Loading)”. ASTM International. http://enterprise.astm.org/filtrexx40.cgi?+REDLINE_PAGES/C78C78M.htm.

———. 2011. “Test Method for Splitting Tensile Strength of Cylindrical Concrete Specimens”. ASTM International. http://enterprise.astm.org/filtrexx40.cgi?+REDLINE_PAGES/C496C496M.htm.

———. 2012. “Practice for Making and Curing Concrete Test Specimens in the Field”. ASTM International. http://enterprise.astm.org/filtrexx40.cgi?+REDLINE_PAGES/C31C31M.htm.

———. 2014a. “Test Method for Compressive Strength of Cylindrical Concrete Specimens”. ASTM International. http://enterprise.astm.org/filtrexx40.cgi?+REDLINE_PAGES/C39C39M.htm.

———. 2014b. “Test Method for Static Modulus of Elasticity and Poissons Ratio of Concrete in Compression”. ASTM International. http://enterprise.astm.org/filtrexx40.cgi?+REDLINE_PAGES/C469C469M.htm.

Concrete Reinforcing Steel Institute. 2001. “Evaluation of Reinforcing Bars in Old Reinforced Concrete Structures”. Engineering Data Report 48.

E28 Committee. 2010. “Practice for Verification and Classification of Extensometer Systems”. ASTM International. http://enterprise.astm.org/filtrexx40.cgi?+REDLINE_PAGES/E83.htm.

———. 2013. “Test Methods for Tension Testing of Metallic Materials”. ASTM International. http://enterprise.astm.org/filtrexx40.cgi?+REDLINE_PAGES/E8E8M.htm.

Gustafson, David P. 2010. “Raising the Grade.” Concrete International 32 (04): 59–62.

Lehman, D., J. Moehle, S. Mahin, A. Calderone, and L. Henry. 2004. “Experimental Evaluation of the Seismic Performance of Reinforced Concrete Bridge Columns.” Journal of Structural Engineering 130 (6): 869–79. doi:10.1061/(ASCE)0733-9445(2004)130:6(869).

Li, Yi-An, Yi-Tong Huang, and Shyh-Jiann Hwang. 2014. “Seismic Response of Reinforced Concrete Short Columns Failed in Shear.” Structural Journal 111 (1-6).

Pham, Thanh Phuong, and Bing Li. 2014. “Seismic Performance of Reinforced Concrete Columns with Plain Longitudinal Reinforcing Bars.” Structural Journal 111 (3): 561–72.

Priestley, Michael John Nigel. 2003. Myths and Fallacies in Earthquake Engineering, Revisited. IUSS press.

Rautenberg, J.M., S. Pujol, and A. Lepage. 2010. “Cyclic Response of Concrete Columns Reinforced with High-Strength Steel.” 9th US National and 10th Canadian Conference on Earthquake Engineering 2010, Including Papers from the 4th International Tsunami Symposium 3 (July). http://nees.org/resources/679/download/2010EQConf-000996.PDF.

Rice, Pual, and David Gustafson. 1976. “Grade 80 Reinforcing Bars and ACI 318-71.” Journal Proceedings 73 (4): 199–206.

Risser, Robert, and Michael Hoffman. 2014. “Turning Billets into Bars.” Concrete Construction. Accessed May 29. http://www.concreteconstruction.net/rebar/turning-billets-into-bars.aspx.

Trejo, David, Andre Barbosa, and Tim Link. 2014. “Seismic Performance of Circular Reinforced Concrete Bridge Columns Constructed with Grade 80 Reinforcement”. Research SRS 500-610. Oregon State University.

Yeh, I-Cheng. 2006. “Generalization of Strength versus Water–cementitious Ratio Relationship to Age.” Cement and Concrete Research 36 (10): 1865–73. doi:10.1016/j.cemconres.2006.05.013.

3.7 ACKNOWLEDGEMENTS

The authors would first like to acknowledge the Oregon Department of Transportation (ODOT) and the Pacific NW Transportation Consortium Region 10 (PacTrans) for providing the funding for this research project. The authors thank Michael Dyson and James Batti for their assistance in fabricating and testing the specimens. Several graduate and undergraduate students participated at some level in this work. They include: Jiaming Chen, Nicolas Matus, Greg Hendrix, Cody Tibbits, Lapyote

Prasittisopin, Yicheng Long, Frank Porter, Amy Kordoska, and Drew Nielson. Their help on this project is truly appreciated. Farwest Steel (Eugene, OR) for assisting with the fabrication of the reinforcement is greatly appreciated. Special thanks to Thomas Murphy and Dennis Lauber from Cascade Steel (McMinnville, OR) for producing a special heat of the Grade 80 steel reinforcement.

3.8 TABLES AND FIGURES

3.8.1 List of Tables

Table 3.1 Experimental test matrix of columns G60, G80, G60-s, and G80-s 62

Table 3.2 Loading profile of columns G60, G80, G60-s, and G80-s..... 62

Table 3.3 Columns G60, G80, G60-s, and G80-s capacities 63

Table 3.4 Summary of columns G60, G80, G60-s, and G80-s ductility values..... 63

Table 3.5 Energy dissipation of columns G60, G80, G60-s, and G80-s..... 63

3.8.2 List of Figures

Figure 3.1 (a) Columns G60, G80, G60-s, and G80-s cross-sections (b) test specimen geometry of columns G60, G80, G60-s, and G80-s.....64

Figure 3.2 Column G60-s & G80-s internal instrumentation 64

Figure 3.3 Column G60-s & G80-s external instrumentation (NTS = not to scale) 65

Figure 3.4 Loading Profile of columns G60, G80, G60-s, and G80-s 65

Figure 3.5 Shear force versus drift ratio of columns G60-s and G80-s 66

Figure 3.6 Shear force versus drift ratio of columns: (a) G60 and G60-s, (b) G80 and G80-s 66

Figure 3.7 Cumulative energy dissipation of columns G60, G80, G60-s, and G80-s ..67

Table 3.1 Experimental test matrix of columns G60, G80, G60-s, and G80-s

Specimen	Moment-shear span ratio	Concrete strength	Longitudinal and transverse reinforcement grade
G60	6	3.59 ksi (24.7 MPa)	Grade 60 ksi (420 MPa)
G80	6	4.66 ksi* (32.1 MPa)*	Grade 80 ksi (550 MPa)
G60-s	3	3.58 ksi (24.65 MPa)	Grade 60 ksi (420 MPa)
G80-s	3	3.85 ksi (26.51 MPa)	Grade 80 ksi (550 MPa)

* Tested data is not available, Abram's Formula with experimental parameter equations determined by Yeh (2006) was used to estimate the concrete strength

Table 3.2 Loading profile of columns G60, G80, G60-s, and G80-s

Drift ratio cycle, %	Number of cycles	Loading rate, in/s (mm/s)	
		G60 & G80	G60-s & G80-s
0.1	3	0.01 (0.25)	0.005 (0.13)
0.2	3	0.01 (0.25)	0.005 (0.13)
0.3	3	0.01 (0.25)	0.005 (0.13)
0.5	3	0.01 (0.25)	0.005 (0.13)
0.7	3	0.01 (0.25)	0.005 (0.13)
0.9	3	0.02 (0.51)	0.01 (0.25)
1.7	3	0.04 (1.0)	0.02 (0.51)
2.6	3	0.08 (2.0)	0.04 (1.0)
3.5	3	0.08 (2.0)	0.04 (1.0)
4.3	3	0.08 (2.0)	0.04 (1.0)
5.2	3	0.08 (2.0)	0.04 (1.0)
6.1	3	0.08 (2.0)	0.04 (1.0)
6.9	3	0.16 (4.1)	0.08 (2.0)

Table 3.3 Columns G60, G80, G60-s, and G80-s capacities

Column	Maximum shear force kip (kN)	Nominal moment capacity, M_n kip-ft (kN-m)	AASHTO plastic moment capacity, M_p kip-ft (kN-m)	Tested moment capacity, M_T kip-ft (kN-m)	Computed overstrength factor, $\lambda_1 = M_T/M_n$	AASHTO overstrength factor, $\lambda_2 = M_p/M_n$
G60	47.9 (213)	463 (628)	554 (751)	631 (856)	1.36	1.20
G80	43.1 (192)	448 (607)	536 (727)	572 (776)	1.28	1.20
G60-s	100.4 (446.6)	463 (628)	554 (751)	629 (853)	1.36	1.20
G80-s	92.0 (409.2)	448 (608)	536 (727)	575 (780)	1.28	1.20

Table 3.4 Summary of columns G60, G80, G60-s, and G80-s ductility values

Specimen	Displacement ductility, μ_Δ		Curvature ductility, μ_ψ			
	Reference yield	First yield	Level 1	Level 2	Level 3	Level 4
G60	4.58	7.00	20.89	19.16*	6.63	2.32
G80	4.35	6.33	23.63	10.21	5.61	1.54
G60-s	4.93	8.88	33.31	7.14	4.46	0.91
G80-s	4.90	7.80	26.86	8.38	2.45	0.74

*Note this large value is believed to have occurred due to the excessive deep spalling on the south side of the column reducing the compressive resistance of the column resulting in larger curvature in this region. It should also be noted this value occurred on the final peak of the 10.00-inch (254mm) displacement cycle shortly prior to column failure.

Table 3.5 Energy dissipation of columns G60, G80, G60-s, and G80-s

	G60	G80	G60-s	G80-s
Energy dissipated at first yield kip-ft (kN-m)	6.43 (8.72)	5.97 (8.09)	4.37 (5.92)	4.57 (6.20)
Energy dissipated at reference yield kip-ft (kN-m)	9.01 (12.2)	8.07 (10.9)	10.39 (14.09)	9.66 (13.10)
Total energy dissipated at column failure kip-ft (kN-m)	684.24 (927.71)	457.67 (620.52)	521.22 (706.68)	377.43 (511.73)

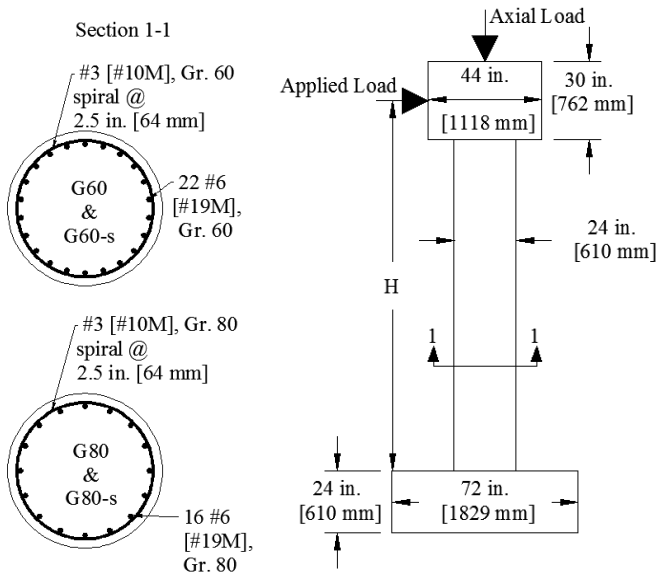

(a) (b)

Figure 3.1 (a) Columns G60, G80, G60-s, and G80-s cross-sections (b) test specimen geometry of columns G60, G80, G60-s, and G80-s

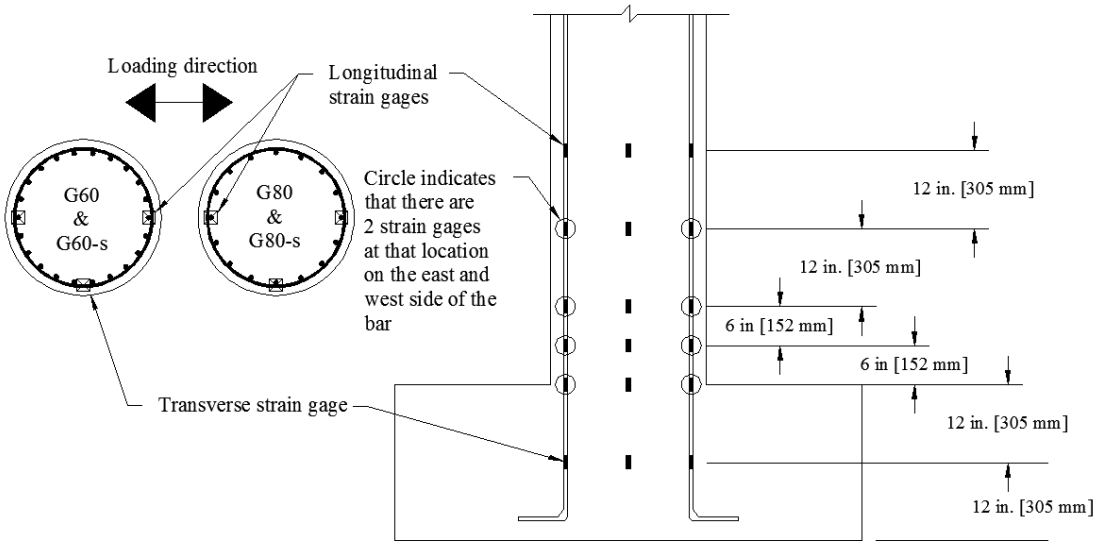

Figure 3.2 Column G60-s & G80-s internal instrumentation

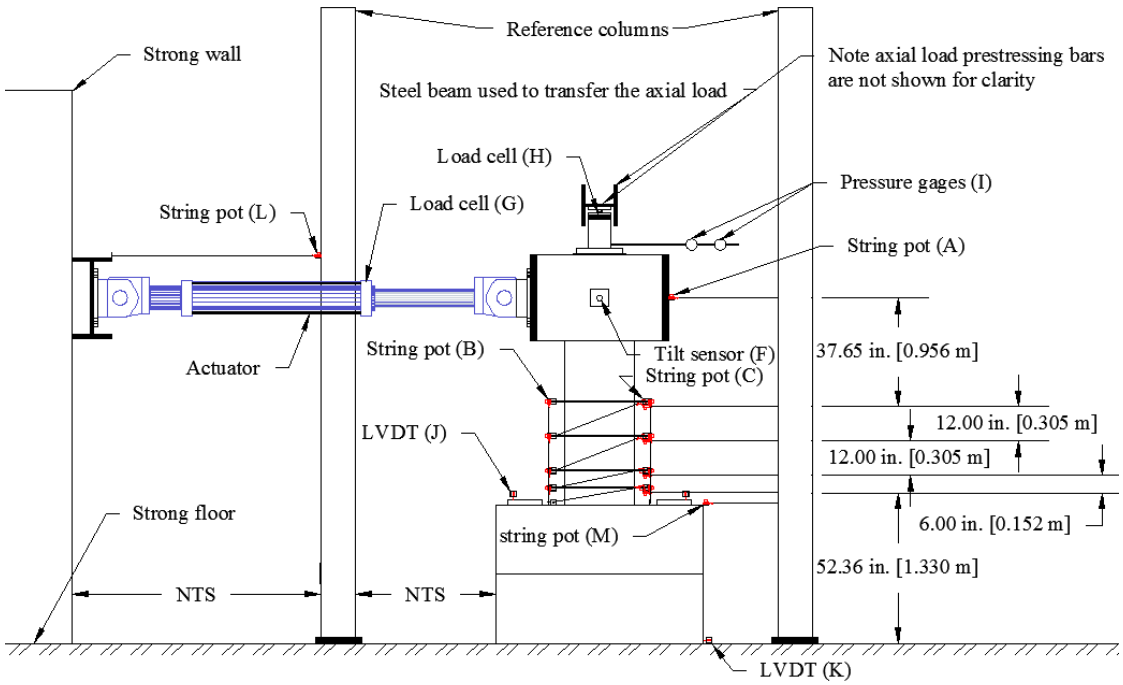

Figure 3.3 Column G60-s & G80-s external instrumentation (NTS = not to scale)

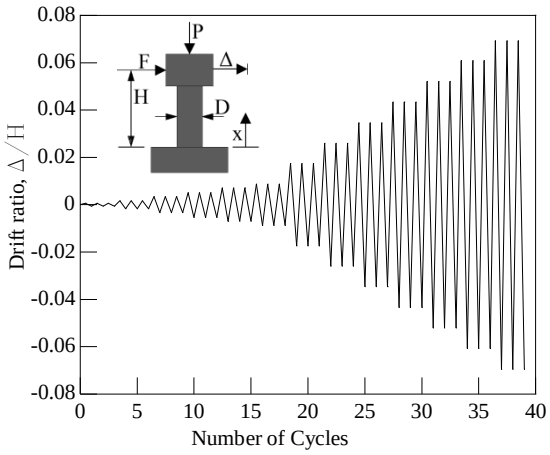

Figure 3.4 Loading Profile of columns G60, G80, G60-s, and G80-s

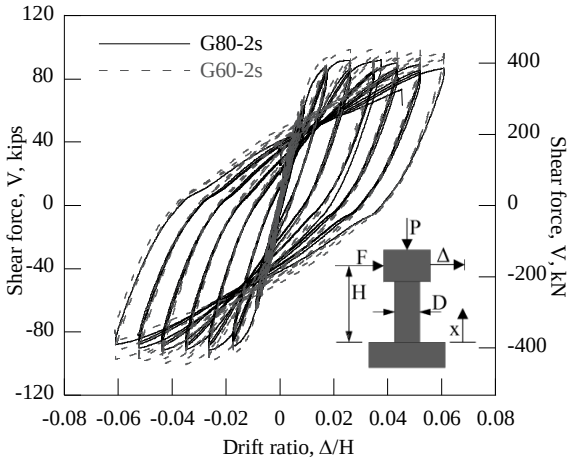

Figure 3.5 Shear force versus drift ratio of columns G60-s and G80-s

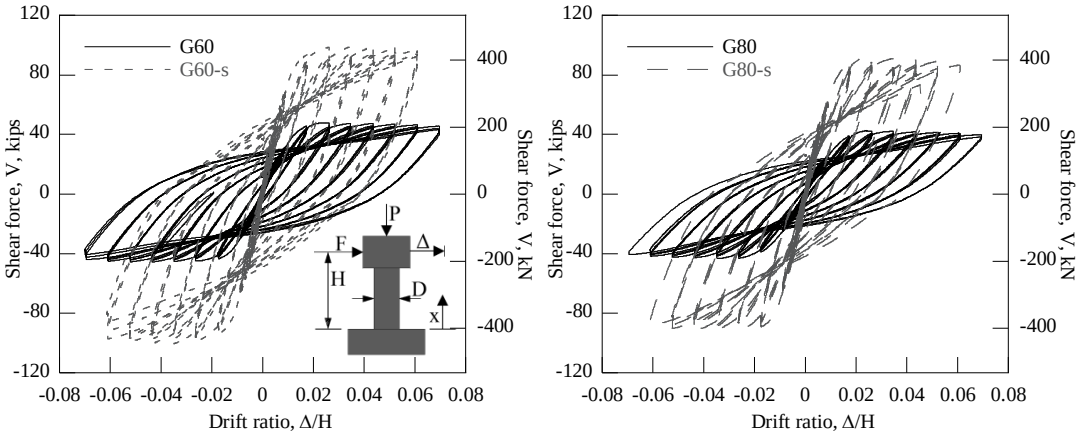

(a) (b)

Figure 3.6 Shear force versus drift ratio of columns: (a) G60 and G60-s, (b) G80 and G80-s

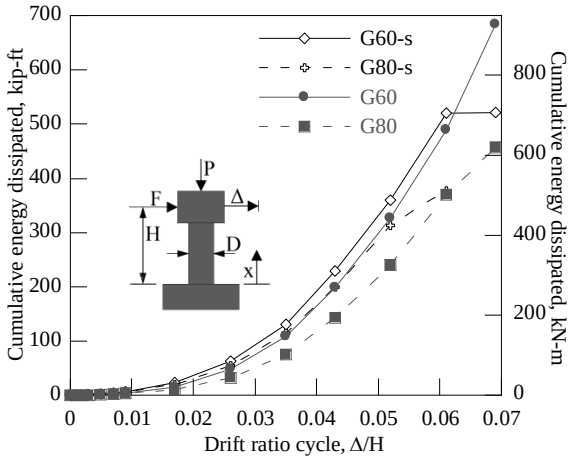

Figure 3.7 Cumulative energy dissipation of columns G60, G80, G60-s, and G80-s

Chapter 4 GENERAL CONCLUSION

As mentioned in Chapters 2 and 3 Grade 80 reinforcement could reduce reinforcement quantities, reduce reinforcement congestion, and improve the constructability and economy of RC bridge columns. However, limited research has been performed to validate the use of Grade 80 reinforcement in RC brige columns. The research presented in Chapter 2 assessed the performance of two pairs of columns, each pair consisting of one column constructed with Grade 60 reinforcement and the other constructed with Grade 80 reinforcement, each pair having similar moment capacities. The goal of Chapter 2 was to determine the effects of the reinforcement grade and the effects of the longitudinal reinforcement ratio on column performance. Chapter 3 assessed the performance of two pairs of columns, each pair consisting of one column constructed with Grade 60 reinforcement and the other constructed with Grade 80 reinforcement, each pair having similar moment capacities. The goal of Chapter 3 was to determine the effects of reinforcement grade and the effects of the moment-shear span ratio (aspect ratio) on column performance.

The main conclusions from the test results presented in Chapters two and three are:

1. All of the columns tested failed due to longitudinal reinforcement bar buckling followed by longitudinal reinforcement bar fracture;
2. Columns constructed with Grade 80 reinforcement achieved similar resistance, maximum drift ratios, and displacement ductility values when compared with the reference columns constructed with Grade 60 reinforcement;

3. Columns constructed with Grade 60 reinforcement exhibited larger hysteretic energy dissipation compare to the columns reinforced with Grade 80 reinforcement. However, by comparing the longitudinal reinforcement ratios ans moment-shear span ratios of columns constructed with Grade 60 and Grade 80 reinforcement agreed with the existing literature that the energy dissipation capacity is a function of the amount of longitudinal reinforcement and column stiffness rather the grade of the reinforcement;
4. Columns constructed with Grade 60 reinforcement typically exhibited larger curvature ductility values compared to the columns reinforced with Grade 80 reinforcement;
5. Columns constructed with Grade 80 reinforcement exhibited smaller computed overstrength factors compared to the columns constructed with Grade 60 reinforcement;
6. The effects of the longitudinal reinforcement ratio on column performance were similar between columns constructed with Grade 80 reinforcement and columns constructed with Grade 60 reinforcement. A key finding was that the increase in the longitudinal reinforcement ratio increased the computed overstrength factor for columns constructed with either Grade 80 or Grade 60 reinforcement;
7. The effects of the moment-shear span ratio (aspect ratio) on column performance were similar between columns constructed with Grade 80 reinforcement and columns constructed with Grade 60 reinforcement. A key

finding was the decrease in the moment-shear span ratio resulted in larger curvature ductility values at the base of the column where the effects of strain penetration affects the curvature and smaller curvature ductility values at higher elevations where the effects of strain penetration do not affect the curvature values.

The results presented in this paper present a promising step towards implementation of Grade 80 reinforcement in the design and construction of RC bridge columns, within the bounds of the variables used in the experimental program. Other parameters outside of the range studied in this paper should be evaluated such as larger longitudinal reinforcement ratios, larger axial loads, and higher concrete strengths. Additionally to remove the effect of the longitudinal reinforcement spacing future testing of columns containing bundled longitudinal reinforcing bars is warranted.

BIBLIOGRAPHY

A01 Committee. 2013. “Test Methods and Definitions for Mechanical Testing of Steel Products”. ASTM International. http://enterprise.astm.org/filtrexx40.cgi?+REDLINE_PAGES/A370.htm.

ASTM. 2009. “A706/A706M-09b Standard Specification for Low-Alloy Deformed and Plain Bars for Concrete Reinforcement.”

Berry, Michael P., and Marc O. Eberhard. 2008. “Performance Modeling Strategies for Modern Reinforced Concrete Bridge Columns”. PEER Report 2007/07. Pacific Earthquake Engineering Research Center. http://peer.berkeley.edu/publications/peer_reports/reports_2007/web_PEER707_BERRYeberhard.pdf.

C09 Committee. 2010. “Test Method for Flexural Strength of Concrete (Using Simple Beam with Third-Point Loading)”. ASTM International. http://enterprise.astm.org/filtrexx40.cgi?+REDLINE_PAGES/C78C78M.htm.

———. 2011. “Test Method for Splitting Tensile Strength of Cylindrical Concrete Specimens”. ASTM International. http://enterprise.astm.org/filtrexx40.cgi?+REDLINE_PAGES/C496C496M.htm.

———. 2012. “Practice for Making and Curing Concrete Test Specimens in the Field”. ASTM International. http://enterprise.astm.org/filtrexx40.cgi?+REDLINE_PAGES/C31C31M.htm.

———. 2014a. “Test Method for Compressive Strength of Cylindrical Concrete Specimens”. ASTM International. http://enterprise.astm.org/filtrexx40.cgi?+REDLINE_PAGES/C39C39M.htm.

———. 2014b. “Test Method for Static Modulus of Elasticity and Poissons Ratio of Concrete in Compression”. ASTM International. http://enterprise.astm.org/filtrexx40.cgi?+REDLINE_PAGES/C469C469M.htm.

Concrete Reinforcing Steel Institute. 2001. “Evaluation of Reinforcing Bars in Old Reinforced Concrete Structures”. Engineering Data Report 48.

E28 Committee. 2010. “Practice for Verification and Classification of Extensometer Systems”. ASTM International. http://enterprise.astm.org/filtrexx40.cgi?+REDLINE_PAGES/E83.htm.

———. 2013. “Test Methods for Tension Testing of Metallic Materials”. ASTM International. http://enterprise.astm.org/filtrexx40.cgi?+REDLINE_PAGES/E8E8M.htm.

Gustafson, David P. 2010. “Raising the Grade.” *Concrete International* 32 (04): 59–62.

Lehman, D., J. Moehle, S. Mahin, A. Calderone, and L. Henry. 2004. “Experimental Evaluation of the Seismic Performance of Reinforced Concrete Bridge Columns.” *Journal of Structural Engineering* 130 (6): 869–79. doi:10.1061/(ASCE)0733-9445(2004)130:6(869).

Li, Yi-An, Yi-Tong Huang, and Shyh-Jiann Hwang. 2014. “Seismic Response of Reinforced Concrete Short Columns Failed in Shear.” *Structural Journal* 111 (1-6).

Mander, J., F. Panthaki, and A. Kasalanati. 1994. “Low-Cycle Fatigue Behavior of Reinforcing Steel.” *Journal of Materials in Civil Engineering* 6 (4): 453–68. doi:10.1061/(ASCE)0899-1561(1994)6:4(453).

Pham, Thanh Phuong, and Bing Li. 2014. “Seismic Performance of Reinforced Concrete Columns with Plain Longitudinal Reinforcing Bars.” *Structural Journal* 111 (3): 561–72.

Priestley, M. J. N., and G. Benzoni. 1996. “Seismic Performance of Circular Columns with Low Longitudinal Reinforcement Ratios.” *ACI Structural Journal* 93 (4): 474–85.

Priestley, Michael John Nigel. 2003. *Myths and Fallacies in Earthquake Engineering, Revisited*. IUSS press.

Rautenberg, J.M., S. Pujol, and A. Lepage. 2010. “Cyclic Response of Concrete Columns Reinforced with High-Strength Steel.” *9th US National and 10th Canadian Conference on Earthquake Engineering 2010, Including Papers from the 4th International Tsunami Symposium* 3 (July). http://nees.org/resources/679/download/2010EQConf-000996.PDF.

Rice, Pual, and David Gustafson. 1976. “Grade 80 Reinforcing Bars and ACI 318-71.” *Journal Proceedings* 73 (4): 199–206.

Risser, Robert, and Michael Hoffman. 2014. “Turning Billets into Bars.” *Concrete Construction*. Accessed May 29. http://www.concreteconstruction.net/rebar/turning-billets-into-bars.aspx.

Rodriguez, M., J. Botero, and J. Villa. 1999. “Cyclic Stress-Strain Behavior of Reinforcing Steel Including Effect of Buckling.” *Journal of Structural Engineering* 125 (6): 605–12. doi:10.1061/(ASCE)0733-9445(1999)125:6(605).

Trejo, David, Andre Barbosa, and Tim Link. 2014. “Seismic Performance of Circular Reinforced Concrete Bridge Columns Constructed with Grade 80 Reinforcement”. Research SRS 500-610. Oregon State University.

Wight, James, and James MacGregor. 2012. *REINFORCED CONCRETE MECHANICS & DESIGN*. 6th ed. Upper Saddle River, New Jersey: Pearson Education, INc.

Yeh, I-Cheng. 2006. “Generalization of Strength versus Water–cementitious Ratio Relationship to Age.” *Cement and Concrete Research* 36 (10): 1865–73. doi:10.1016/j.cemconres.2006.05.013.